(Received 19 September 2024, Accepted 29 November 2024, Scheduled 11 December 2024)

Free Space Transmission Lines in Receiving Antenna Operation

Reuven Ianconescu[1,*] and Vladimir Vulfin[2]

[1] Department of Electrical Engineering, Shenkar College of Engineering and Design, Ramat Gan, Israel
[2] Electromagnetics Infinity LTD, Israel

ABSTRACT: This work derives exact expressions for the voltage and current induced into a two conductors non-isolated transmission line by an incident plane wave. The methodology is to use the transmission line radiating properties to derive scattering matrices and make use of reciprocity to derive the response to the incident wave. This methodology to derive receiving characteristics from the radiation properties via a scattering matrix is novel, and we already started to implement it to additional cases. An immediate advantage we obtained from this method is the derivation of a very simple analytic expression for the voltage and current for a matched transmission line. The analysis is in the frequency domain, and it considers transmission lines of any small electric cross section, incident by a plane wave from any direction and polarization. The analytic results are validated by successful comparison with ANSYS commercial software simulation results, and compatible with other published results.

1. INTRODUCTION

In a previous work [1], we made a full analysis of the radiation properties of transmission lines (TLs), including radiated field intensity and polarization, radiation pattern, radiation resistance, and more. The analysis has been carried out for a forward or backward wave separately, and for any combination of them as well.

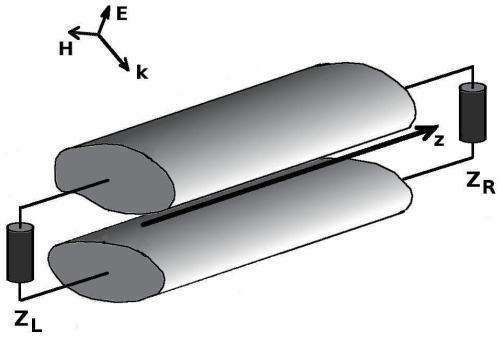

FIGURE 1. Configuration of a two ideal conductors transmission line (TL), connected at both sides to passive loads: Z_L (left) and Z_R (right), hit by a monochromatic plane wave propagating toward the centre of coordinates. The cross section is electrically small and may be of any shape. The loads are located at the terminations of the TL, and are shown farther away, due to technical drawing limitations. We consider the most general case, so that the plane wave hits from any arbitrary direction.

In the current work, we investigate the inverse problem of a TL connected to passive (lumped) loads absorbing electromagnetic power, namely we calculate the voltage and differential current (amplitude and phase) developed on a two-conductors TL hit by a monochromatic plane wave, as shown in Figure 1. Similar to [1], we consider an ideal lossless TL of any small electric cross section.

A more detailed look at the incident plane wave and its polarization is given in Figure 2. It propagates toward the coordinates origin with phase $e^{-j\mathbf{k}\cdot\mathbf{r}}$, so that the wavenumber vector $\mathbf{k} = -\hat{\mathbf{r}}k$ points toward the origin. Expanding $\hat{\mathbf{r}}$ in Cartesian unit vectors, the phase can be written as

$$e^{jk[x\sin\theta\cos\varphi + y\sin\theta\sin\varphi + z\cos\theta]}, \tag{1}$$

where θ and φ are the spherical angles which represent the direction of the plane wave incidence. The plane wave travels toward the centre of coordinates, perpendicular to the θ, φ plane, with a polarization angle α from the θ axis, so that the E field at the origin, where its phase is defined to be 0 (see Eq. (1)), is given by

$$\mathbf{E} = E_0(\hat{\boldsymbol{\theta}}\cos\alpha + \hat{\boldsymbol{\varphi}}\sin\alpha) \tag{2}$$

or its components

$$E_\theta = E_0\cos\alpha; \quad E_\varphi = E_0\sin\alpha. \tag{3}$$

The configuration as defined here is a scattering problem, requiring a full wave solution to set the tangential component of

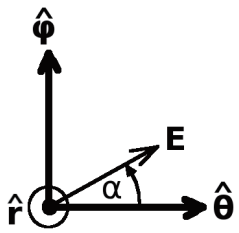

FIGURE 2. The incident plane wave propagates toward the centre of coordinates in the $-\hat{\mathbf{r}}$ direction. In spherical coordinates the local equiphase surface is θ, φ and the polarization is at angle α from the θ axis, so that at the origin the E field is given by Eq. (2). This is the most general case of linear polarisation.

* Corresponding author: Reuven Ianconescu (riancon@gmail.com).

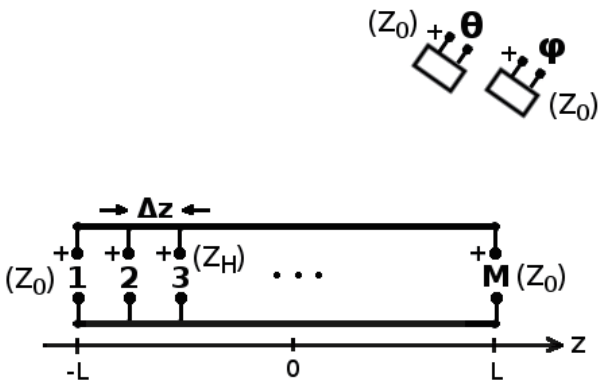

FIGURE 3. Circuit with M parallel ports along the TL at distances Δz (see Eq. (4)) and two additional ports representing far antennas matched for the $\hat{\boldsymbol{\theta}}$ and $\hat{\boldsymbol{\varphi}}$ polarizations. The two additional ports $M+1$ and $M+2$ are named as θ and φ. We name $\mathbf{S}_V$ as the scattering matrix for this circuit, defined for the TL impedance Z_0 at ports 1,M, θ, φ and for a high impedance $Z_H \to \infty$ at the middle ports $2 \ldots M-1$, as indicated.

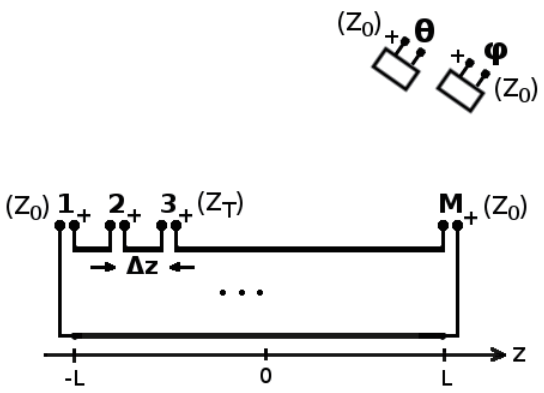

FIGURE 4. Circuit with M serial ports along the TL at distances Δz and two additional ports representing far antennas matched for the $\hat{\boldsymbol{\theta}}$ and $\hat{\boldsymbol{\varphi}}$ polarizations, named θ and φ. We name $\mathbf{S}_I$ as the scattering matrix for this circuit, defined for the TL impedance Z_0 at ports 1,M, θ, φ and for a tiny impedance $Z_T \to 0$ at the middle ports $2 \ldots M-1$.

the electric field to 0 on the surface of the TL. However, we derive here an analytic solution to this problem, which is compared with a full wave HFSS (high-frequency structure simulator) solution. Such analytic solution is made possible with the aid of the circuits shown in Figures 3 and 4, on which we set "artificial" ports in the middle of the transmission line (parallel in Figure 3 and serial in Figure 4). Another "trick" is the choice of the characteristic impedances. The characteristic impedances of the parallel ports in Figure 3 are very high ($Z_H \to \infty$), so that a matched port is an open circuit, mimicking the natural state of the circuit. Similarly, the characteristic impedances of the serial ports in Figure 4 are tiny ($Z_T \to 0$) so that a matched port is shorted. Due to this choice, the incoming voltage/current at a matched port in Figures 3/4 represents the voltage/current at the given location of the port.

The derivation of the voltage induced into the TL is based on the circuit shown in Figure 3. Using our detailed knowledge of the field radiated by such TL [1], we derive the scattering matrix for this circuit, and using its reciprocity we find the voltage induced by an incident plane wave. The response to a θ or φ polarized plane wave is found by exciting the system with a voltage at the θ or φ ports.

Similarly, the derivation of the induced current is based on the circuit shown in Figure 4. In both circuits, the ports locations z_n and the separation Δz are given by:

$$\Delta z = \frac{2L}{M-1}; \quad z_n = -L + (n-1)\Delta z, \tag{4}$$

but their scattering matrices are *different*. For the circuit in Figure 3, we define the matrix $\mathbf{S}_V$ (V = voltages), and for the circuit in Figure 4, we define the matrix $\mathbf{S}_I$ (I=currents). Those matrices satisfy

$$\mathbf{V}^- = \mathbf{S}_V \mathbf{V}^+; \quad \mathbf{I}^- = \mathbf{S}_I \mathbf{I}^+, \tag{5}$$

where $\mathbf{V}^+$, $\mathbf{V}^-$ are column vectors of incoming and outgoing voltages for the circuit in Figure 3, and $\mathbf{I}^+$, $\mathbf{I}^-$ are column vectors of incoming and outgoing currents for the circuit in Figure 4. Both matrices are defined for the TL impedance Z_0 at ports 1, M, θ, and φ, while $\mathbf{S}_V$ is defined for high impedance $Z_H \to \infty$ at the middle ports $2 \ldots M-1$ (Figure 3), and $\mathbf{S}_I$ is defined for tiny impedance $Z_T \to 0$ at the middle ports $2 \ldots M-1$ (Figure 4).

Although Figures 3 and 4 describe different systems, their far ports θ and φ are common, and being defined for Z_0 at both systems, they satisfy the relations:

$$V_\theta^+ = Z_0 I_\theta^+; \quad V_\varphi^+ = Z_0 I_\varphi^+ \tag{6}$$

More technical details on our derivation are given in Subsection 2.2.

A problem similar to this one has been handled in [2–6], but not for an arbitrary cross section (as in Figure 1), and not for a general incident plane wave (as in Figure 2). The methodology used in these works is based on a generalization of the telegraph equations for transmission lines, by which one adds induced voltage and current sources derived from the incident plane wave, to the RLCG model of the TL. An alternative approach of using voltage sources along the TL induced by the z component of the incident electric field and voltage sources at the terminations induced by the x component of this field has been published in [7], again for the private case of a twin lead. We show in this work that our results are fully compatible with those obtained in [2–7], and we shall therefore summarize the induced sources methodology in Subsection 2.3.

The advantages and novelties of our derivation are:

- The method of using S matrix reciprocity to derive receiving characteristics from transmitting characteristics is original and may be extended to additional configurations.
- Unlike [2–7], we do not restrict ourselves to wires which are thin relative to the distance between them, presenting a more general algorithm, i.e., applicable to more realistic configurations.

- Our formulation is for a general incident plane wave, i.e., from an arbitrary direction θ, φ, and arbitrary polarization α.
- In our formulation we first obtain a (simpler) solution for matched TL and further generalize it for any passive loads.
- From the matched solution, the connection between the radiation and receiving properties of TL emerges naturally.
- In other methods it is not evident how a (simpler) solution for matched TL is generalizable to the non-matched case, in spite of the fact that the induced sources are independent of the termination loads.
- The previous works [2–7] did not inquire the relations and reciprocity between the receiving and radiation, although references on radiation from TL were available, e.g., [15]. This work emphasises those relations, uses them for interpretation, and summarises the reciprocity in Section 7.

The work is organized as follows. For the reader easy to follow the manuscript, a glossary of abbreviations and a summary of the main results is given in Subsection 2.1. In Subsection 2.2, we explain the methodology used in this work to derive the voltage and current along a TL hit by a monochromatic plane wave. Because the methodology of obtaining receiving characteristics from radiation characteristics via S parameters has not been extensively used in the past, we give here a detailed description of this methodology. In Subsection 2.3, we detail the alternative "induced sources" methodology used in [2–6] and explain the sufficient conditions to show the compatibility of our results with this method.

In Section 3, we carry out all the analytic derivations for the voltage and differential current along a TL hit by a monochromatic plane wave. We start with the voltage on a TL with matched loads and generalize the result for a TL terminated in any loads (Z_L and Z_R, as in Figure 1). Those calculations use the far E field radiated from TL (based on [1] and summarized in Appendix A) and the properties of the generalized scattering matrix, summarized in Appendix B.

In Section 4, we describe the full wave HFSS simulations performed and explain some delicate issues regarding the measurements of voltage and current. It is mentioned that a TL hit by a monochromatic plane wave may develop common mode currents. However, our derivation of the current is based on the reciprocity of the system defined in Figure 4. The currents used to define the scattering matrix are differential, and for those differential currents we use the far fields developed in [1]. Hence, when we use the reciprocity to express the current developed on the TL as a function of the plane wave excitation, we obtain only the differential part of the current, and this drawback applies also to the methods used in [2–7]. If the purpose is to calculate the power on the loads, this is not a limitation, because the common mode does not affect this power (see comment in page 3 of [7]), only this has to be taken into account in the current measurement in Section 4. Regarding this issue, we want to emphasize that for power on the loads one only needs the voltages, and we calculate the differential currents for completeness and proof of concept.

In Subsection 5.1, we validate the analytic results with full wave HFSS simulations for a cross section which is not a twin lead, showing that this formalism works for a general electrically small cross section. We compare the theoretical results obtained in Section 3 for the voltage and differential current with full wave HFSS solutions for matched and non-matched transmission lines. In Subsection 5.2, we prove that the analytic results obtained in Section 3 are fully compatible with the results obtained in [2–7]. In Section 6, we calculate general expressions for the powers transferred to the loads and interpret them in terms of the transmission radiation patterns in [1] and incident plane wave polarization. We show that the power in the "left" load is closely related to the transmitting properties of a source at the left termination and vice-versa. In Section 7, we show a full analysis of the connection between the radiation characteristics of TL calculated in [1] and the receiving characteristics calculated in this work.

The work is ended with some concluding remarks.

Note: through this work, the phasor amplitudes are RMS values, hence there is no 1/2 in the expressions for power. Also, it is worthwhile to mention that the results of this work depend on physical sizes relative to the wavelength and hence are valid for all frequencies satisfying the condition of small electric cross section.

2. PRELIMINARIES

2.1. Glossary and Main Results

We summarize in Table 1 some abbreviations used in this work and the main results of the manuscript.

2.2. S Parameters Methodology

We explain in detail in this subsection the S parameters method used to obtain the response to an incident plane wave. To derive the S parameters for either the circuit in Figure 3 or 4, we need to calculate the far electric field radiated by the TL, using the formalism developed in [1].

We first note that the characteristic impedance Z_0 of the TL and an equivalent separation distance d can be found by an electrostatic cross section analysis, leading to a twin lead equivalent (examples for determining Z_0 and d are shown in Appendix B of [1]). The twin lead equivalent is shown in Figure 5. When the TL is excited at its port(s), this equivalent twin lead radiates the same far fields as the actual TL. To emphasize, we *do not* solve for the twin lead geometry, but for an arbitrary cross section in Figure 1, so that the twin lead is only used as an intermediate tool for the calculations.

As shown in [1], the radiated far fields are proportional to this separation distance d. Hence, we expect the voltage response of the TL in receiving mode also proportional to this separation distance d, for a given incident field E_0 (see Eqs. (2), (3) and Figure 2). We therefore normalize the scattering matrices for the circuits in Figures 3 and 4, so that an incoming excitation at port θ or φ (named V_θ^+ and V_φ^+) represents the components of the incident field E_θ and E_φ in Eq. (3), multiplied by the

TABLE 1

TL	transmission line
double-matched	TL matched on both terminations
$V(z)$, $I(z)$	Voltage and current solutions on double-matched TL Eqs. (30), (38)
$\Delta V(z)$, $\Delta I(z)$	Voltage and current correction terms due to non matching Eqs. (43), (51)
$V_{\text{NM}}(z)$	Voltage for the general (non matched) case: $V(z)+\Delta V(z)$
$I_{\text{NM}}(z)$	Current for the general (non matched) case: $I(z)+\Delta I(z)$
P_L	Power on "left" load for double-matched TL Eq. (90)
P_R	Power on "right" load for double-matched TL Eq. (91)
$P_{\text{NM,L}}$	Power on "left" load general case Eq. (97)
$P_{\text{NM,R}}$	Power on "right" load general case Eq. (98)

equivalent separation distance d, as follows:

$$V^+ \equiv E_0\, d, \tag{7}$$

or by components (equivalent to Eq. (3)):

$$V_\theta^+ = V^+ \cos\alpha; \quad V_\varphi^+ = V^+ \sin\alpha. \tag{8}$$

The normalization procedure allowing the above equivalence is explained in Appendix A.

As mentioned in the Introduction, the $\mathbf{S}_V$ describing the circuit in Figure 3 is defined for the TL impedance Z_0 at ports 1, M, θ, φ and for a high impedance $Z_H \to \infty$ at the *middle* ports $2 \ldots M-1$. To first obtain the voltages on double-matched TL, we match all TL ports (1 and M with Z_0 and the middle ports are open) so that $V^+ = 0$ at those ports. Now exciting the θ and φ ports with adequate excitations V_θ^+, V_φ^+ (according to Eq. (8)), we obtain the outgoing voltages (which are the total voltages) on all the TL ports by:

$$V_n^- = \sum_{i=1}^{M+2} S_{V_{n,i}} V_i^+ = S_{V_{n,\theta}} V_\theta^+ + S_{V_{n,\varphi}} V_\varphi^+ \equiv V_{\text{matched}} \tag{9}$$

and given that Δz is arbitrarily small (or M arbitrarily large) this results in the voltage as a function of z along the double-matched TL for the given incident plane wave. Hence to obtain the voltage on the double-matched TL, we need only the (n,θ) and (n,φ) elements of $\mathbf{S_V}$ (for $1 \le n \le M$)).

To generalize this for a TL with any terminations, we remark that the middle ports are still matched (with $Z_H \to \infty$, i.e., open) so we need two additional incoming voltages from ports 1 and M in the summation (9):

$$V_n^- = V_{\text{matched}} + S_{V_{n,1}} V_1^+ + S_{V_{n,M}} V_M^+ \equiv V_{\text{matched}} + \Delta V \tag{10}$$

Similarly, to obtain the current induced on a TL, we carry out the same procedure with the $\mathbf{S_I}$ matrix elements. As mentioned in the Introduction, the $\mathbf{S}_I$ describing the circuit in Figure 4 is defined for the TL impedance Z_0 at ports 1, M, θ, φ and for a tiny impedance $Z_T \to 0$ at the *middle* ports $2 \ldots M-1$. This choice allows the representation of a double-matched TL by matching ports 1 and M with Z_0 and the middle ports shorted, yielding the current on the double-matched TL (similar to (9)):

$$I_n^- = \sum_{i=1}^{M+2} S_{I_{n,i}} I_i^+ = S_{I_{n,\theta}} I_\theta^+ + S_{I_{n,\varphi}} I_\varphi^+ \equiv I_{\text{matched}}, \tag{11}$$

and the generalization for a TL with any terminations:

$$I_n^- = I_{\text{matched}} + S_{I_{n,1}} I_1^+ + S_{I_{n,M}} I_M^+ \equiv I_{\text{matched}} + \Delta I \tag{12}$$

The full derivation of the voltage and current and the necessary scattering matrices elements is carried out in Section 3.

2.3. Induced Sources Methodology

As discussed in the Introduction, the problem of a TL hit by an incident plane wave has been previously handled in [2–6] using the induced sources methodology. We explain here this method and discuss the conditions needed to show our compatibility with its results. In this subsection *only*, the voltage V and current I are general and do not refer specifically to the double-match case.

The method consists in a generalization of the telegraph equations for transmission lines. Given C' and L' the capacitance and inductance per unit length, using $Z_0 = \sqrt{L'/C'}$ and the identity $\sqrt{L'C'} = 1/c$, we write the (inhomogeneous) telegraph equations in the following compact form

$$\frac{dV}{dz} + jk(Z_0 I) = V_s \tag{13}$$

$$Z_0 \frac{dI}{dz} + jkV = Z_0 I_s \tag{14}$$

where we identify for $V_s = 0$ and $I_s = 0$ the "usual" homogeneous telegraph equations, used when the TL is only excited at its termination port(s).

Here, the source terms V_s and I_s are induced by the H_y and E_x fields of the incident plane wave, integrated along the x axis of the twin lead (see Figure 5), as follows:

$$V_s(z) = jk\eta_0 \int_0^d H_y(x,z)dx \simeq jk\eta_0 H_y(z) d \tag{15}$$

$$Z_0 I_s(z) = -jk \int_0^d E_x(x,z)dx \simeq -jkE_x(z)d, \tag{16}$$

and $\eta_0 = 377\,[\Omega]$ is the free space impedance. Please note that Eqs. (13) and (14) (together with (15) and (16)) are identical to Eqs. (10) and (13) in [2].

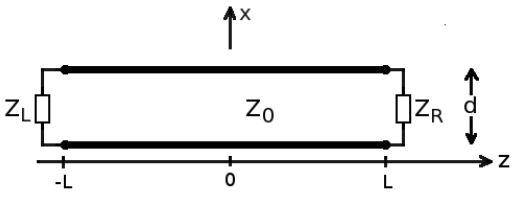

FIGURE 5. Twin lead equivalent of the analysed transmission line, defined by the separation distance d between the conductors, and the characteristic impedance Z_0, both computed by the cross section analysis described in Appendix B of [1]. The TL is of length $2L$.

It is important here to remark that the integration over the range d is strictly valid only for the twin lead geometry shown in Figure 5, which is the only cross section geometry handled in [2–7]. As shown in [1], one can use a twin lead *equivalent* for any cross section geometry, provided that it is of small electric size. Therefore, the last ($\simeq$) parts of Eqs. (15) and (16) are consistent with our framework dealing with any cross section geometry which is restricted to a small electric size ($kd \ll 1$), so that d is the *equivalent* separation.

The coupled non-homogeneous differential Eqs. (13) and (14) can be decoupled into two second order equations:

$$\frac{d^2V}{dz^2} + k^2V = \frac{dV_s}{dz} - jk(Z_0 I_s) \tag{17}$$

$$Z_0\frac{d^2I}{dz^2} + k^2 Z_0 I = Z_0\frac{dI_s}{dz} - jkV_s \tag{18}$$

In [2], the authors wrote the general solution for those second order differential equations, subject to the termination conditions:

$$V(-L) = -Z_L I(-L); \quad V(L) = Z_R I(L), \tag{19}$$

however they used, in the expression for the sources, the implicit assumption that the incident field has only a H_y component.

In the introduction of [3], the author mentions that: *The results in [1] (i.e., Taylor, in this work [2]), albeit often referenced, are less-often used directly since, in the form presented, they are somewhat complex and difficult to interpret physically.* Hence, [3] presents a somehow simplified solution, but even this solution subject to general termination conditions (19) is complicated, and it is not obvious in this method how one first gets a simpler solution for double-matched TL, which is *physically interpretable*, as we show in this work.

Noting that the induced source terms V_s and I_s are independent of the loads Z_L and Z_R, and given that we first obtain a (simpler) solution for the double-matched TL, it will be **sufficient** to show that the *double-matched* solution satisfies Eqs. (13) and (14).

This is done in Subsection 5.2, where we also show that the mismatch correction terms $\Delta V(z)$ and $\Delta I(z)$ (see Subsection 2.1) satisfy the homogeneous telegraph equations.

3. DERIVATION OF THE VOLTAGE AND DIFFERENTIAL CURRENT ALONG THE TL

In this section, we derive the S matrices for the circuits in Figures 3 and 4, (named $\mathbf{S}_V$ and $\mathbf{S}_I$, respectively) and from them find the voltage and current along the TL.

As explained in Section 2.2, to find the voltage/current on a double-matched TL, one needs only the cross elements between the group of ports $1 \ldots M$ and group θ, φ of the S matrices, i.e., (n,θ) and (n,φ), and we therefore start with this part in the following subsection.

3.1. Voltage and Current along a Double-Matched TL

To derive the matrix elements (n,θ) and (n,φ), we calculate the matrix elements (θ,n) and (φ,n), and use reciprocity. For this, we need the θ and φ components of the far E field radiated from the circuits in Figures 3 and 4 fed at port n, with all other ports matched. This configuration is shown in Figures 6 and Figure 7 for the calculation of $\mathbf{S}_V$ and $\mathbf{S}_I$, respectively. For both circuits, we define the lengths from port n to the terminations:

$$l_1 = z_n + L; \quad l_2 = L - z_n, \tag{20}$$

and the middle points z_{m_1}, z_{m_2}:

$$z_{m_1} = -l_2/2; \quad z_{m_2} = l_1/2, \tag{21}$$

Given that all other ports (except n) are matched, the circuits develop a forward wave **only** in the region $[z_n, L]$ and a backward wave only in the region $[-L, z_n]$, shown schematically in the figures. Hence, the feeding source at port n "sees" an impedance Z_0 from each side of the TL. The difference between the circuits is the sign of the backward wave in the region $[-L, z_n]$: negative in Figure 6 and positive in Figure 7.

For $\mathbf{S}_V$, we need to calculate the far E field radiated by the circuit in Figure 6. Using the results in [1], summarized in Eqs. (A1) and (A2) for a forward and backward wave, respectively, we set into Eqs. (A1) $I^+ \to \frac{V_n^+}{Z_H} e^{-jkl_2/2} e^{jkz_{m_2}\cos\theta}$ and $2L \to l_2$, and into Eqs. (A2) $I^- \to -\frac{V_n^+}{Z_H} e^{-jkl_1/2} e^{jkz_{m_1}\cos\theta}$ and $2L \to l_1$. Adding the results yields the far E field:

$$\eta_0 G(r) 2kd \frac{V_n^+}{Z_H}[(f_1 - f_2)\hat{\boldsymbol{\theta}}\cos\varphi - (f_1 + f_2)\hat{\boldsymbol{\varphi}}\sin\varphi], \tag{22}$$

where the functions f_1 and f_2 are defined as:

$$f_1 \equiv e^{-jk(l_1 + l_2\cos\theta)/2}\sin(kl_1\cos^2(\theta/2))$$

$$f_2 \equiv e^{-jk(l_2 - l_1\cos\theta)/2}\sin(kl_2\sin^2(\theta/2)), \tag{23}$$

and we note that the port n to which the field (22) is related is given indirectly by the values of $l_{1,2}$.

The functions $f_{1,2}$ in (23), presented via $l_{1,2}$ are functions of z by setting $z_n = z$ in (20). The values of those functions at the terminations are $f_1(-L) = f_2(L) = 0$, while $f_2(-L)$ and $f_1(L)$ are directly proportional to the effective antenna lengths $\mathbf{l}_{\text{eff}}^{\pm}$ related to radiation by a forward or backward wave or in receiving mode related to the left or right ports at $z = \mp L$, as will become clear in Section 7.

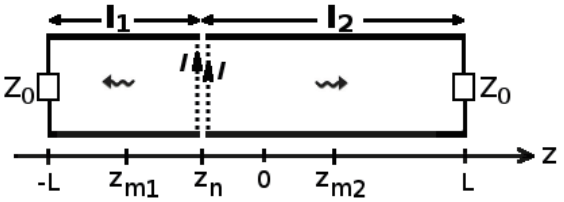

FIGURE 6. The circuit described in Figure 3 while fed at the middle port n by V_n^+ and matched at all other ports. Defining $I \equiv V_n^+/Z_H$, we get two "separate" TLs, the one between $[z_n, L]$ carrying a forward wave $Ie^{-jk(z-z_n)}$ and the one between $[-L, z_n]$ carrying a backward wave $-Ie^{jk(z-z_n)}$.

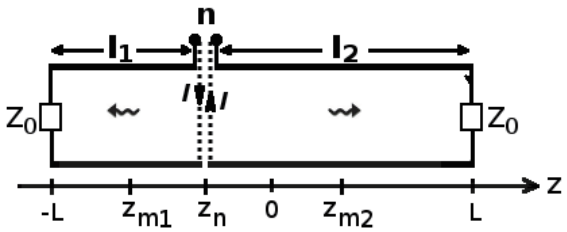

FIGURE 7. The circuit described in Figure 4 while fed at the middle port n by I_n^+ and matched at all other ports. Defining $I \equiv I_n^+ Z_T/Z_0$, we get two "separate" TLs, the one between $[z_n, L]$ carrying a forward wave $Ie^{-jk(z-z_n)}$ and the one between $[-L, z_n]$ carrying a backward wave $Ie^{jk(z-z_n)}$.

Separating the E field into θ and φ components and scaling with Eq. (A7), we obtain the outgoing voltage waves

$$V_\theta^- = jV_n^+(Z_0/Z_H)[f_2 - f_1]\cos\varphi \quad (24)$$
$$V_\varphi^- = jV_n^+(Z_0/Z_H)[f_1 + f_2]\sin\varphi. \quad (25)$$

Results (24) and (25) define the (θ, n) and (φ, n) elements for $\mathbf{S}_V$, respectively. For the columns $1 < n < M$:

$$S_{V_{\theta,\,1<n<M}} = j(Z_0/Z_H)[f_2 - f_1]\cos\varphi \quad (26)$$
$$S_{V_{\varphi,\,1<n<M}} = j(Z_0/Z_H)[f_1 + f_2]\sin\varphi. \quad (27)$$

For column $n = 1$ or M, the results are similar, only replace $\frac{Z_0}{Z_H}$ by 1. The transpose elements are found by the reciprocity condition $S_{i,j}Z_j = S_{j,i}Z_i$ (see Appendix B, Eq. B8), where Z_i and Z_j are the impedances for which ports i and j have been defined, respectively. Given that the ports 1, M, θ, and φ are defined for Z_0 of the TL and that ports $2 \ldots M-1$ are defined for Z_H, the transposed relations $S_{n,\theta}$ and $S_{n,\varphi}$ are given by Eqs. (26) and (27), under the replacement $\frac{Z_0}{Z_H} \to 1$:

$$S_{V_{n,\theta}} = j[f_2 - f_1]\cos\varphi \quad (28)$$
$$S_{V_{n,\varphi}} = j[f_1 + f_2]\sin\varphi. \quad (29)$$

Now using Eqs. (8) and (9), we obtain the voltage on the double-matched TL:

$$V(z) = jV^+[f_2(z)\cos(\varphi - \alpha) - f_1(z)\cos(\varphi + \alpha)] \quad (30)$$

Eq. (30) is the final result for the voltage on a double-matched TL, and let us get some physical meaning of it. As previously explained, $f_2(-L)$ and $f_1(L)$ are proportional to the effective antenna lengths $\mathbf{l}_{\text{eff}}^{\pm}$ related in receiving mode to the left or right ports at $z = \mp L$. The $\cos(\varphi \mp \alpha)$ terms are the polarisation mismatch of the incident field, as will become evident in Sections 6 and 7, for example, if we look for a maximum voltage at $z = -L$, $f_1 = 0$ so that only $f_2 \propto \mathbf{l}_{\text{eff}}^{+}$ plays a role. Such a case is shown in Section 5, Figure 11. Next we go on with the current.

For $\mathbf{S}_I$, we go through a similar procedure for the circuit in Figure 7. Using Eqs. (A1) and (A2) for a forward and backward wave, respectively, we set into Eqs. (A1) $I^+ \to \frac{I_n^+ Z_T}{Z_0} e^{-jkl_2/2} e^{jkz_{m_2}\cos\theta}$ and $2L \to l_2$, and into Eqs. (A2) $I^- \to \frac{I_n^+ Z_T}{Z_0} e^{-jkl_1/2} e^{jkz_{m_1}\cos\theta}$ and $2L \to l_1$. Adding the results yields the far E field:

$$-\eta_0 G(r) 2kd \frac{I_n^+ Z_T}{Z_0}[(f_1+f_2)\hat{\boldsymbol{\theta}}\cos\varphi + (f_2+f_1)\hat{\boldsymbol{\varphi}}\sin\varphi], \quad (31)$$

where the functions f_1 and f_2 are defined in Eq. (23). Scaling with Eq. (A8) we obtain:

$$I_\theta^- = -jI_n^+(Z_T/Z_0)[f_1 + f_2]\cos\varphi \quad (32)$$
$$I_\varphi^- = jI_n^+(Z_T/Z_0)[f_1 - f_2]\sin\varphi, \quad (33)$$

from which we find the $\mathbf{S}_I$ matrix elements for the columns $1 < n < M$:

$$S_{I_{\theta,\,1<n<M}} = -j(Z_T/Z_0)[f_1 + f_2]\cos\varphi \quad (34)$$
$$S_{I_{\varphi,\,1<n<M}} = j(Z_T/Z_0)[f_1 - f_2]\sin\varphi \quad (35)$$

For column $n = 1$ or M, the results are similar, only replace $\frac{Z_T}{Z_0}$ by 1. The transpose elements are found by the reciprocity condition $S_{i,j}Z_i = S_{j,i}Z_j$ (see Appendix B, Eq. B13), where Z_i and Z_j are the impedances for which ports i and j have been defined, respectively. Note that this reciprocity condition is different from the one used for the voltage calculation. Given that the ports 1, M, θ, and φ are defined for Z_0 of the TL and that ports 2 ... $M-1$ are defined for Z_T, the transposed relations $S_{n,\theta}$ and $S_{n,\varphi}$ are given by Eqs. (34) and (35) under the replacement $\frac{Z_T}{Z_0} \to 1$:

$$S_{I_{n,\theta}} = -j[f_1 + f_2]\cos\varphi \quad (36)$$
$$S_{I_{n,\varphi}} = j[f_1 - f_2]\sin\varphi \quad (37)$$

Now using Eq. (11) and the relations (6), (8), we obtain the current along the double-matched TL:

$$I(z) = -j(V^+/Z_0)[f_1(z)\cos(\varphi+\alpha) + f_2(z)\cos(\varphi-\alpha)] \quad (38)$$

It is easy to check that Eqs. (30) and (38) satisfy the termination conditions (19) with $Z_L = Z_R = Z_0$.

3.2. Voltage and Current along a TL with Arbitrary Loads

To generalize the results (30) and (38) for arbitrary loads connected at the terminations of the TL, we need additional elements of the matrices $\mathbf{S}_V$ and $\mathbf{S}_I$, specifically the elements $(i, 1)$ and (i, M), where $1 \le i \le M$, as shown in Eqs. (10) and (12).

For the calculation of $\mathbf{S}_V$, port $i = 1$ or M is fed by the incoming voltage V_i^+, "seeing" a total impedance Z_0, so that

$V_i^- = 0$, i.e., both ports are matched. On the TL a forward/backward wave only arises for $i = 1, M$ respectively. Hence, the outgoing voltage at port n is $V_i^+ e^{-jk|z_n - z_i|}$, specifically: $V_i^+ e^{-jkl_1}$ for $n = 1$ and $V_i^+ e^{-jkl_2}$ for $n = M$, resulting in

$$S_{V_{1\le n\le M,\ i=1,M}} = \begin{cases} e^{-jkl_1} & i = 1 \text{ and } n \neq i \\ e^{-jkl_2} & i = M \text{ and } n \neq i \\ 0 & n = i \end{cases} \tag{39}$$

where the value of n is "hidden" in the values of $l_{1,2}$. As explained in Section 2.2, in this configurations all $V^+ = 0$ at the middle ports $1...M-1$ because those are matched, and we need only to express V_1^+ and V_M^+ to set them in Eq. (10).

We define the reflection coefficients Γ_L (at the left side) and Γ_R (at the right side):

$$\Gamma_L = \frac{Z_L - Z_0}{Z_L + Z_0} \text{ and } \Gamma_R = \frac{Z_R - Z_0}{Z_R + Z_0}. \tag{40}$$

so that:

$$V_1^+ = \Gamma_L V_1^- \text{ and } V_M^+ = \Gamma_R V_M^-, \tag{41}$$

Setting them in Eq. (10)

$$V_n^- = S_{V_{n,1}} \Gamma_L V_1^- + S_{V_{n,M}} \Gamma_R V_M^- + V(z) \tag{42}$$

where $V(z)$ is the double-matched solution in Eq. (30), and V_n^- is the outgoing voltage at port n, which is also the total voltage for $1 < n < M$, because at those ports $V^+ = 0$. Therefore, at least for the middle ports (and there we can replace $S_{V_{n,1}} = e^{-jkl_1}$ and $S_{V_{n,M}} = e^{-jkl_2}$):

$$\Delta V(z) = e^{-jkl_1} \Gamma_L V_1^- + e^{-jkl_2} \Gamma_R V_M^-, \tag{43}$$

is the correction term due to non matching, but we will show that (43) is valid for all z.

To find V_1^- and V_M^-, we set $n = 1$ and $n = M$ in Eq. (42), obtaining:

$$V_1^- = \Gamma_R V_M^- e^{-jk2L} + V(-L), \tag{44}$$
$$V_M^- = \Gamma_L V_1^- e^{-jk2L} + V(L). \tag{45}$$

The solution of the above two equations for V_1^- and V_M^- yields:

$$V_1^- = \frac{\Gamma_R e^{-j2kL} V(L) + V(-L)}{1 - \Gamma_L \Gamma_R e^{-j4kL}} \tag{46}$$

$$V_M^- = \frac{\Gamma_L e^{-j2kL} V(-L) + V(L)}{1 - \Gamma_L \Gamma_R e^{-j4kL}}. \tag{47}$$

Coming back to the correction term (43), we find that the sum of (30) and (43): $V(z) + \Delta V(z)$ reduces to $(\Gamma_L + 1)V_1^-$ for $z = -L$ (i.e., the voltage at port 1) and reduces to $(\Gamma_R + 1)V_M^-$ for $z = L$ (i.e., the voltage at port M); therefore Eq. (43) is applicable everywhere on the TL. Hence, the "non-matched" voltage on the TL is

$$V_{\text{NM}}(z) = V(z) + \Delta V(z), \tag{48}$$

where $\Delta V(z)$ is the correction term due to non matching, given in Eq. (43) to be added to the double-matched solution (30). This concludes the voltage developed on the TL due to a monochromatic plane wave.

For the calculation of $\mathbf{S}_I$, port $i = 1$ or M is fed by the incoming current I_i^+, "seeing" a total impedance Z_0, so that $I_i^- = 0$, i.e., both ports are matched. On the TL a forward/backward wave only arises for $i = 1, M$ respectively. Hence, the outgoing current at port n is $I_i^+ e^{-jk|z_n - z_i|}$, specifically: $I_i^+ e^{-jkl_1}$ for $n = 1$ and $I_i^+ e^{-jkl_2}$ for $n = M$. Therefore, the matrix elements for $S_{I_{1\le n\le M\ i=1,M}}$ are *identical* to the ones for $\mathbf{S}_V$ in Eq. (39).

The difference is in the sign of the reflected waves at the non-matched ports 1 and M:

$$I_1^+ = -\Gamma_L I_1^- \text{ and } I_M^+ = -\Gamma_R I_M^-, \tag{49}$$

Setting them in Eq. (12)

$$I_n^- = -S_{I_{n,1}} \Gamma_L I_1^- - S_{I_{n,M}} \Gamma_R I_M^- + I(z) \tag{50}$$

where $I(z)$ is the double-matched solution in Eq. (38), and I_n^- is the outgoing current at port n, which is also the total current for $1 < n < M$, because at those ports $I^+ = 0$. Therefore, for the middle ports, where we can replace $S_{I_{n,1}} = e^{-jkl_1}$ and $S_{I_{n,M}} = e^{-jkl_2}$, we obtain:

$$\Delta I(z) = -e^{-jkl_1} \Gamma_L I_1^- - e^{-jkl_2} \Gamma_R I_M^-, \tag{51}$$

which is the correction term due to non-matching, and as in the case of the voltage, it is valid for all z.

To find I_1^- and I_M^- we set $n = 1$ and $n = M$ in Eq. (50) and obtain two equations analogous to (44) and (45), which yield a solution similar to (46) and (47), by replacing $\Gamma \to -\Gamma$:

$$I_1^- = \frac{-\Gamma_R e^{-j2kL} I(L) + I(-L)}{1 - \Gamma_L \Gamma_R e^{-j4kL}} \tag{52}$$

$$I_M^- = \frac{-\Gamma_L e^{-j2kL} I(-L) + I(L)}{1 - \Gamma_L \Gamma_R e^{-j4kL}}. \tag{53}$$

Hence, the "non-matched" current on the TL is

$$I_{\text{NM}}(z) = I(z) + \Delta I(z), \tag{54}$$

where $\Delta I(z)$ is the correction term due to non-matching, given in Eq. (51) to be added to the double-matched solution (38).

The "non-matched" solutions (48) and (54) satisfy the termination conditions (19). This concludes the current developed on the TL due to a monochromatic plane wave.

4. FULL WAVE HFSS SIMULATIONS

We describe in this Section the HFSS simulations done for the scattering problem defined in Figure 1. The results of these simulations are compared in the next section with the analytic results for voltage and current. When we simulate the transmission line, measuring the current on the conductors and the voltage between conductors due to plane wave excitation, we take the following steps to obtain accurate results:

- The ANSYS HFSS simulation uses an adaptive solver, so we check for convergence. Specifically, we require two consecutive convergences below the threshold to confirm that the solution is stable and not diverging.
- To calculate the current and voltage, we draw lines (a closed loop for current and a line between the conductors

for voltage). To obtain more accurate results, we build dummy vacuum objects with a dense mesh and place the lines inside these vacuum objects. This ensures that the simulation is more precise in the area of current and voltage calculation.

- In addition to the default convergence criteria, we also converge the values of current and voltage separately to ensure stability.

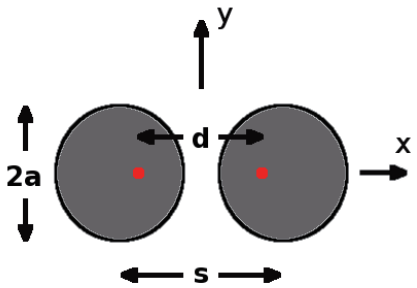

FIGURE 8. Cross section of two parallel cylinders: the distance between the centres is $s = 3.59$ cm, and the diameters are $2a = 2.54$ cm. The red points show the current images which define the twin lead representation, and the distance between them $d = 2.537$ cm is calculated in Eq. (55).

We used a non twin lead cross section (used also in [1]), shown in Figure 8. For this cross section one knows analytically the distance d in the twin lead representation (shown as red points in Figure 8) by image theory, yielding

$$d = \sqrt{s^2 - (2a)^2} = 2.537\text{cm}, \tag{55}$$

and also the characteristic impedance

$$Z_0 = \frac{\eta_0}{\pi} \ln\left(\frac{d+s}{2a}\right) = 105.6\,\Omega \tag{56}$$

while for other cross sections those can be determined by an electrostatic ANSYS 2D Maxwell simulation, as shown in Appendix B of [1].

The electric field of a plane wave is by default $E_0 = 1$ V/m in the HFSS simulation, so to normalize the results for $V^+ = E_0\, d = 1$ V (see Eq. 7) we divide the measured results by the value of d in Eq. (55).

For convenience, we shall use a fixed TL length of $l \equiv 2L = 125$ cm and test for different frequencies. We measure the voltage and current along the TL from $z = -61.25$ cm to $z = 61.25$ cm at intervals of 6.125 cm, in total at 21 points. At the TL terminations $z = -L$ and $z = L$, we use inactive lumped ports defined for the impedance we need at those terminations.

Two-conductors transmission lines excited *only* at terminations develop the transverse electromagnetic (TEM) mode, so that both E_z and H_z are 0. In such a case, one can measure the voltage by $\int \mathbf{E} \cdot \mathbf{dl}$ from the "+" to the "−" conductor and the current using $\oint \mathbf{H} \cdot \mathbf{dl}$ around the "+" conductor, both on *any* integration path.

In the case analyzed here, the TL is excited by an external plane wave; therefore, depending on the incidence of this wave E_z and/or H_z are not necessarily 0, we need more careful definitions for the voltage and current measurements, as described in the following subsections.

4.1. Voltage Measurement

The voltage measured by the integral $\int \mathbf{E} \cdot \mathbf{dl}$ in the cross section depends on the chosen integration path if $H_z \neq 0$, as shown in Figure 9. To define the correct path, we look at the definitions of the parallel ports in Figure 3. Those have been defined on the x-z plane, so that *only* x directed currents flow through the port, and this fact has been used in the calculation of the S matrix in Section 3, see Figure 6.

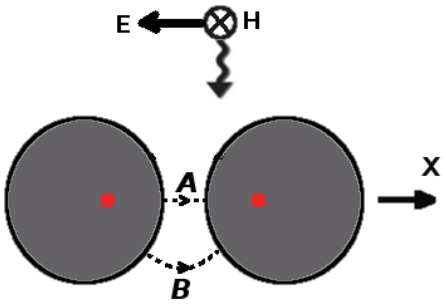

FIGURE 9. Cross section voltage measurement on two possible pathes A and B. In case $H_z = 0$, all pathes lead to the same result, namely $\int_A \mathbf{E} \cdot \mathbf{dl} = \int_B \mathbf{E} \cdot \mathbf{dl}$. However, if $H_z \neq 0$, as for the incident plane wave shown here, the result of the path integral depends on the paths used, and the correct voltage measurement is $\int_A \mathbf{E} \cdot \mathbf{dl}$, i.e., along the x axis consistent with the parallel ports definition in Figure 3.

Therefore, to be consistent with the parallel ports definition, the correct path to measure the voltage is path A (on the x axis) shown in Figure 9, and this path is used in all the voltage measurements in Section 5.

4.2. Current Measurement

For the case $E_z = 0$, the current can be measured by $\oint \mathbf{H} \cdot \mathbf{dl}$ around the "positive" conductor, on any integration path, like path C in Figure 10. In the opposite case consisting in an incident plane wave for which $E_z \neq 0$ (as shown in the figure), not only the integration path has to be tight around the conductor, but also, due to common mode current, one has to measure

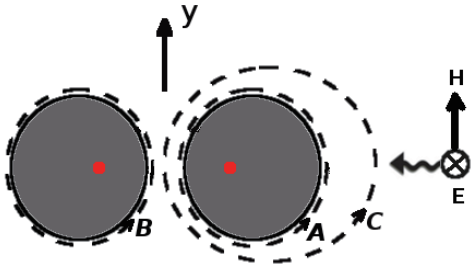

FIGURE 10. Cross section differential current measurement for the case $H_z \neq 0$ requires integration on tight loops around each conductor from which one obtains the currents I_A and I_B (Eq. (57)). The differential current is calculated in Eq. (58).

around both conductors, on paths A and B, as shown in Figure 10, to obtain the currents

$$I_A = \oint_A \mathbf{H}\cdot\mathbf{dl}; \quad I_B = \oint_B \mathbf{H}\cdot\mathbf{dl}. \tag{57}$$

As mentioned in the Introduction, our analytic results for currents represent differential currents; therefore to compare the HFSS simulation results to the analytic results, we calculate the simulation differential current:

$$I = (I_A - I_B)/2; \tag{58}$$

If $E_z = 0$, I_B trivially reduces to $-I_A$, so that the differential current is the current on the "positive" conductor, which may be calculated by integrating on any path around it, like path A or C in Figure 10.

5. VALIDATION OF THE ANALYTIC RESULTS

5.1. Comparisons with HFSS Full Wave Solution

5.1.1. Double-Matched Transmission Line

We validate in this section the analytic results for a double-matched TL in Eqs. (30) and (38) by comparison with full wave solution of ANSYS HFSS simulation results, described in the previous section.

We analyze three examples, each from a main incidence direction, by plane waves traveling along the x, y, or z axes. In all examples, the incident electric field intensity satisfies $Ed = \eta_0 Hd = 1$ V. The half length of the TL is $L = 0.625$ m (or the length $2L = 1.25$ m).

In the first example, we examine a plane wave traveling from $\theta = \pi$, along the z axis, colinear with the TL, having the phase e^{-jkz}, as shown in Figure 11. For $\theta = \pi$, Eqs. (30) and (38) (normalised by Z_0) reduce to

$$V(z) = V^+ je^{-jkL}\sin[k(L-z)]\cos(\varphi-\alpha) \tag{59}$$
$$Z_0 I(z) = -V^+ je^{-jkL}\sin[k(L-z)]\cos(\varphi-\alpha), \tag{60}$$

Clearly, at $\theta = \pi$, the angle φ is ill defined and so is the polarisation angle α (Figure 2), but the difference $\varphi - \alpha$ is meaningful. The maximum voltage and current occur at $\alpha = \varphi$ or $\pi - \varphi$, representing two opposite polarisations. Choosing $\alpha = \varphi$ the polarisation in Figure 2 becomes $\hat{\boldsymbol{\theta}}\cos\varphi + \hat{\boldsymbol{\varphi}}\sin\varphi$, which equals $-\hat{x}$ as shown in Figure 11, and using $V^+ = 1$ V Eqs. (59) and (60) become

$$V(z) = je^{-jkL}\sin[k(L-z)] \tag{61}$$
$$Z_0 I(z) = -je^{-jkL}\sin[k(L-z)], \tag{62}$$

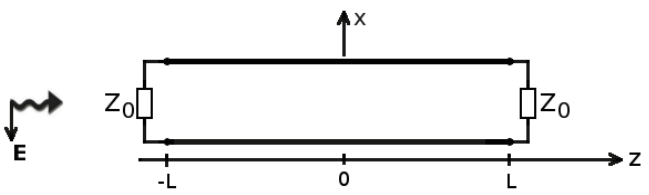

FIGURE 11. Matched TL illuminated by a $-\hat{\mathbf{x}}$ polarised plane wave from $\theta = \pi$.

which behave oscillatory according to the frequency, with 0 value at right termination at $z = L$. We remark that for this plane wave $E_z = H_z = 0$ therefore the voltage and current can be measured on any paths (see Figures 9 and 10).

Figures 12–14 show the voltage and normalised current for the $-\hat{\mathbf{x}}$ polarised plane wave from $\theta = \pi$ in Figure 11 for frequencies 30, 60, and 120 MHz, or $L/\lambda = 1/16$, 1/8, and 1/4, respectively. The voltage at the left termination at $z = -L$ is $V(-L) = je^{-jkL}\sin(2kL)$, resulting in $0.27 + j0.65$, $(1+j)/\sqrt{2}$ and 0 for the cases $L/\lambda = 1/16$, 1/8, and 1/4, respectively. The normalised currents $Z_0 I(-L)$ get the minus of the above values, satisfying the termination condition $V(-L) = -Z_0 I(-L)$.

In the next example, we use a plane wave hitting from $\theta = \varphi = \pi/2$ with phase e^{jky} as shown in Figure 15. For this direction, Eqs. (30) and (38) (normalised by Z_0) reduce to

$$V(z) = V^+\sin\alpha[1 - e^{-jkL}\cos(kz)] \tag{63}$$
$$Z_0 I(z) = jV^+\sin\alpha\, e^{-jkL}\sin(kz), \tag{64}$$

The maximum voltage and current are obtained for $\alpha = \pm\pi/2$. We use $\alpha = \pi/2$, yielding a $\hat{\boldsymbol{\varphi}}$ polarisation, which equals $-\hat{x}$ in this case (as shown in Figure 15). We note that this is the same plane wave shown in Figure 9, so that here the path on which one measures the voltage matters: it must be path A in Figure 9.

Using $V^+ = 1$ V and $\alpha = \pi/2$ in Eqs. (63) and (64) results in

$$V(z) = 1 - e^{-jkL}\cos(kz) \tag{65}$$
$$Z_0 I(z) = je^{-jkL}\sin(kz), \tag{66}$$

Figures 16–18 show the voltage and normalised current for the $-\hat{x}$ polarised plane wave from $\theta = \pi/2$ and $\varphi = \pi/2$ in Figure 11 for frequencies 30, 60, and 120 MHz, or $L/\lambda = 1/16$, 1/8, and 1/4, respectively.

As expected, the voltage is an even function of z and the current an odd function of z. Specifically, the voltages at the terminations at $z = -L$ and L are $0.146 + j0.354$, $0.5 + j0.5$ and 1 for the cases $L/\lambda = 1/16$, 1/8, and 1/4, respectively. The normalised currents have the same values at $z = L$, satisfying the termination condition $V(L) = Z_0 I(L)$, and minus the above values at $z = -L$, satisfying $V(-L) = -Z_0 I(-L)$.

The voltages in the middle of the TL at $z = 0$ are $0.076 + j0.383$, $1 - 1/\sqrt{2} + j/\sqrt{2}$ and $1 + j$ for the cases $L/\lambda = 1/16$, 1/8, and 1/4, respectively, and the current at $z = 0$ is of course 0.

In the next example, we use a plane wave incident from $\theta = \pi/2$ and $\varphi = 0$, with phase e^{jkx} as shown in Figure 19. For this direction, Eqs. (30) and (38) (normalised by Z_0) reduce to

$$V(z) = -jV^+\cos\alpha\, e^{-jkL}\sin(kz) \tag{67}$$
$$Z_0 I(z) = -V^+\cos\alpha[1 - e^{-jkL}\cos(kz)]. \tag{68}$$

Here, the maximum is obtained for $\alpha = 0$ or π. Using $\alpha = \pi$ defines, according to Figure 2, a $-\hat{\boldsymbol{\theta}}$ polarisation which equals $\hat{z}$ at $\theta = \pi/2$ and $\varphi = 0$, as shown in Figure 19. This is the same plane wave mentioned in Figure 10, which requires current measurement by integrating on the tight trajectories A and

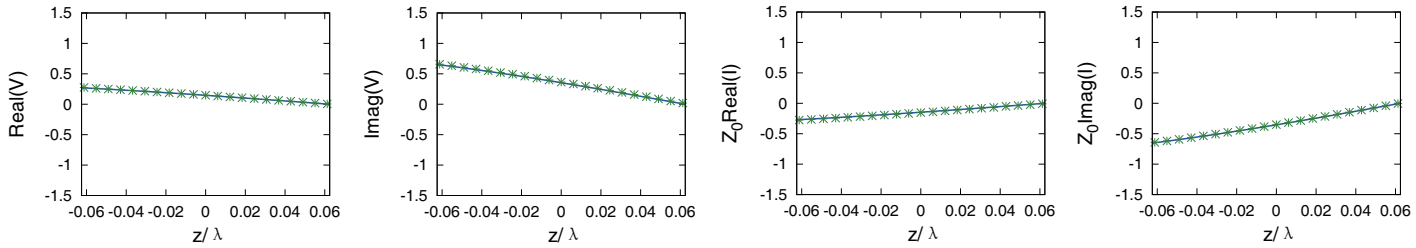

FIGURE 12. Real and imaginary parts of the voltage $V(z)$ and normalised current $Z_0 I(z)$ for the plane wave incidence shown in Figure 11, at frequency 30 MHz or $L/\lambda = 1/16$. The continuous line is the analytic solution in Eqs. (61) and (62) and the stars are the ANSYS simulation results.

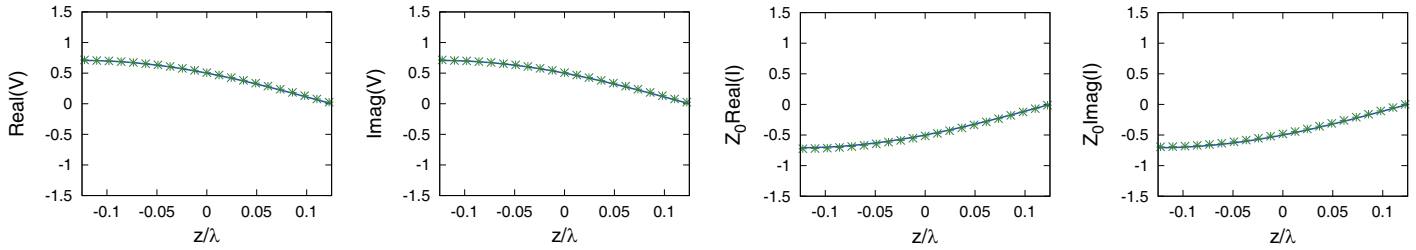

FIGURE 13. Same as Figure 12, for frequency 60 MHz or $L/\lambda = 1/8$.

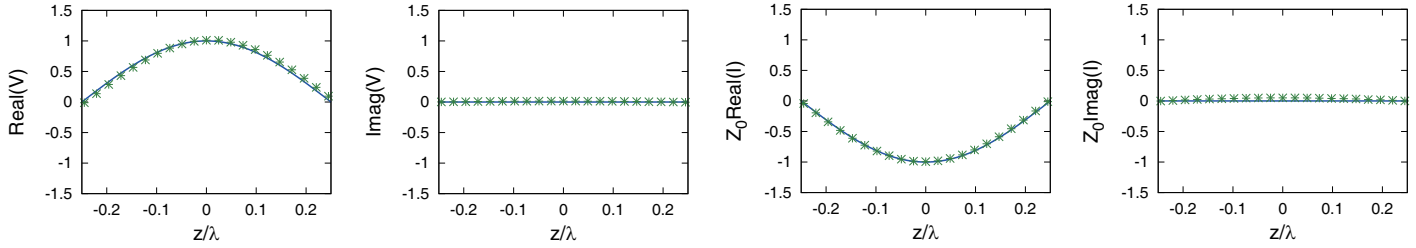

FIGURE 14. Same as Figure 12, for frequency 120 MHz or $L/\lambda = 1/4$.

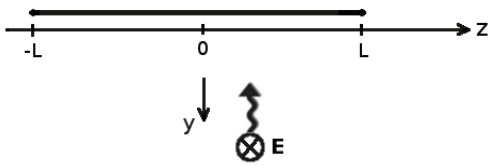

FIGURE 15. Matched TL illuminated by a $-\hat{x}$ polarised plane wave from $(\theta = \pi/2, \varphi = \pi/2)$ (as also shown in Figure 9). The view is from the positive x axis direction, so that only the "upper positive" conductor is seen.

B in Figure 10, using Eq. (58) to determine the differential current.

Using $V^+ = 1\,\text{V}$ and $\alpha = \pi$ in Eqs. (63) and (64) results in

$$V(z) = je^{-jkL}\sin(kz) \tag{69}$$
$$Z_0 I(z) = 1 - e^{-jkL}\cos(kz), \tag{70}$$

Figures 20–22 show the voltage and normalised current for the $\hat{z}$ polarised plane wave from $\theta = \pi/2$ and $\varphi = 0$ in Figure 19 for frequencies 30, 60, and 120 MHz, or $L/\lambda = 1/16$, 1/8, and 1/4, respectively.

As expected, the voltage is an odd function of z and the current an even function of z. The voltage developed for the incident field in Figure 19 (Eq. 69) has the value of the normalised current developed for the incident field in Figure 15 (Eq. 66) and vice versa.

5.1.2. Non Matched Transmission Line

We compare here several unmatched cases for the $-\hat{x}$ polarised plane wave from $\theta = \pi/2$ and $\varphi = \pi/2$, shown in Figure 15 for frequency 60 MHz. The double-matched solutions are given in Eqs. (65) and (66), and for this frequency ($kL = \pi/4$) are:

$$V(z) = 1 - e^{-j\pi/4}\cos(kz) \tag{71}$$
$$Z_0 I(z) = je^{-j\pi/4}\sin(kz), \tag{72}$$

as shown in Figure 17.

We generalize them for non-matched cases using Eqs (48) and (54), obtaining the correction terms due to non-matching (Eqs. (43) and (51))

$$\Delta V(z) = \frac{\Gamma_L e^{-jkz} + \Gamma_R e^{jkz} - 2j\Gamma_L\Gamma_R\cos(kz)}{\sqrt{2}(1+\Gamma_R\Gamma_L)} \tag{73}$$

$$Z_0\Delta I(z) = \frac{\Gamma_L e^{-jkz} - \Gamma_R e^{jkz} - 2\Gamma_L\Gamma_R\sin(kz)}{\sqrt{2}(1+\Gamma_R\Gamma_L)} \tag{74}$$

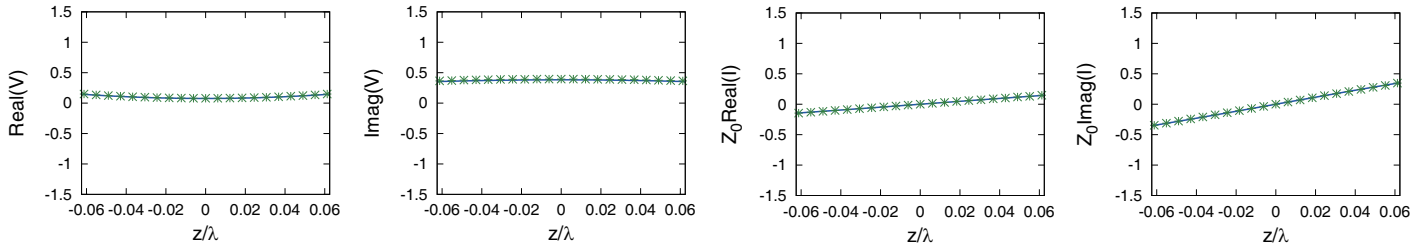

FIGURE 16. Real and imaginary parts of the voltage $V(z)$ and normalised current $Z_0 I(z)$ for the plane wave incidence shown in Figure 15, at frequency 30 MHz or $L/\lambda = 1/16$. The continuous line is the analytic solution in Eqs. (65) and (66) and the stars are the ANSYS simulation results.

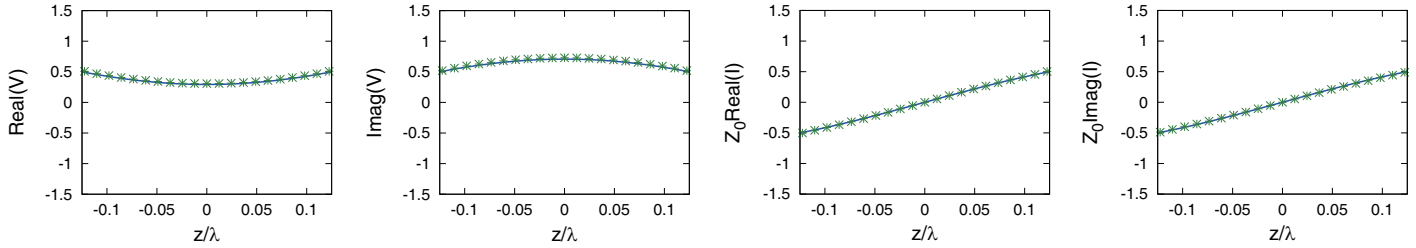

FIGURE 17. Same as Figure 16, for frequency 60 MHz or $L/\lambda = 1/8$.

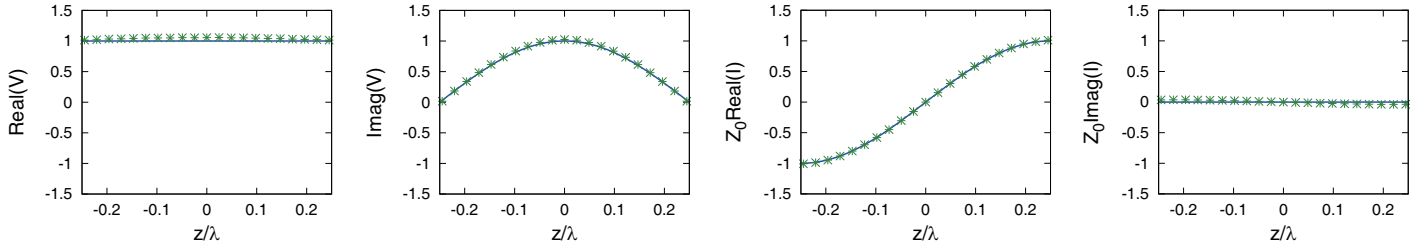

FIGURE 18. Same as Figure 16, for frequency 120 MHz or $L/\lambda = 1/4$.

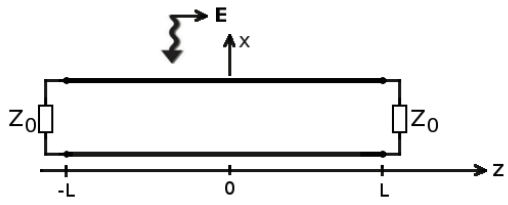

FIGURE 19. Matched TL illuminated by a $\hat{\mathbf{z}}$ polarised plane wave from $(\theta = \pi/2, \varphi = 0)$ (as also shown in Figure 10).

Figures 23–25 show the voltage and normalised current for the cases: $Z_L = Z_0/2$ and $Z_R = 2Z_0$, $Z_L = Z_R = Z_0/2$ and $Z_L = Z_R = 2Z_0$, respectively.

5.2. Compatibility with Previous Works

We show in this subsection that our analytic results are compatible with the results obtained by other authors [2–7]. Given that they solved for the induced sources as defined in Eqs. (13) and (14) (identical to Eqs. (10) and (13) in [2]), it is enough to show that our analytic solution satisfies (13) and (14).

It is easy to check that the correction for unmatched TL, ΔV in (43) and ΔI in (51), satisfies the homogeneous telegraph equations Eqs. (13) and (14), hence

$$\frac{d\Delta V}{dz} + jk(Z_0 \Delta I) = 0; \quad Z_0 \frac{d\Delta I}{dz} + jk\Delta V = 0, \tag{75}$$

which is clear, because the induced sources depend only on the incident field and not on the loads.

Therefore (as mentioned in Section 2.3), *it is enough to show* that Eqs. (13) and (14) are satisfied by the double-matched solution $V(z)$, $I(z)$ in Eqs. (30), (38), for a general incident plane wave.

First, we need the phase of the incident plane wave (Eq. (1)) on the TL at $x \simeq 0$, $y = 0$, and $-L \le z \le L$, which comes out

$$e^{jkz\cos\theta}, \tag{76}$$

so the incident E_x and H_y fields along the TL are

$$E_x(z) = E_x e^{jkz\cos\theta}; \quad H_y(z) = H_y e^{jkz\cos\theta}, \tag{77}$$

where the values E_x and H_y are understood as the values at the origin. Using the unit vectors identity $\hat{\mathbf{x}} = \hat{\mathbf{r}}\sin\theta\cos\varphi + \hat{\boldsymbol{\theta}}\cos\theta\cos\varphi - \hat{\boldsymbol{\varphi}}\sin\varphi$, given that the incident E field has only θ and φ components, the x component of the electric field (at origin) is

$$\begin{aligned} E_x &= E_\theta \cos\theta\cos\varphi - E_\varphi \sin\varphi \\ &= E_0(\cos\alpha\cos\theta\cos\varphi - \sin\alpha\sin\varphi) \end{aligned} \tag{78}$$

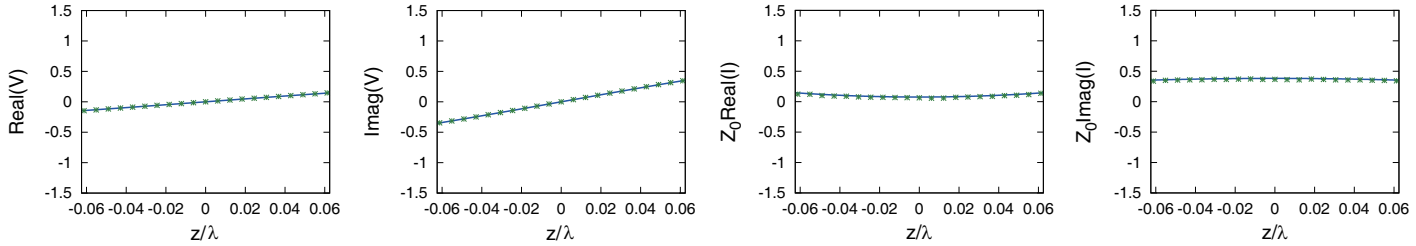

FIGURE 20. Real and imaginary parts of the voltage $V(z)$ and normalised current $Z_0 I(z)$ for the plane wave incidence shown in Figure 19, at frequency 30 MHz or $L/\lambda = 1/16$. The continuous line is the analytic solution in Eqs. (69) and (70) and the stars are the ANSYS simulation results.

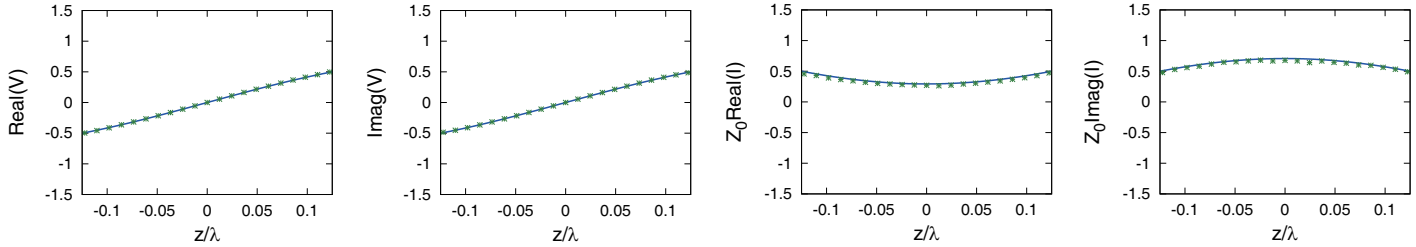

FIGURE 21. Same as Figure 20, for frequency 60 MHz or $L/\lambda = 1/8$.

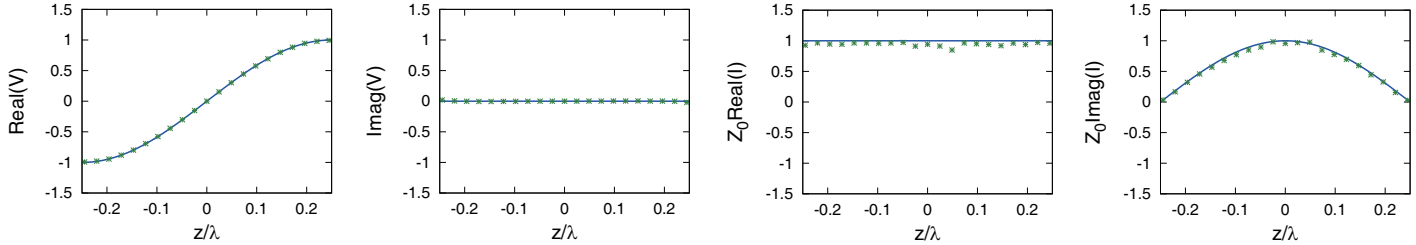

FIGURE 22. Same as Figure 20, for frequency 120 MHz or $L/\lambda = 1/4$.

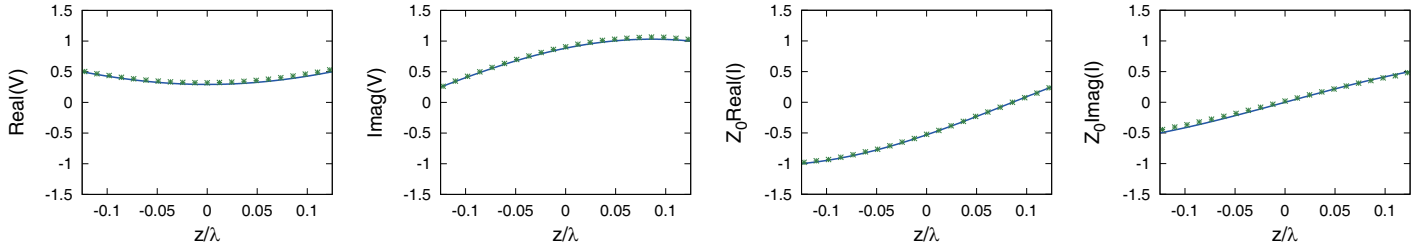

FIGURE 23. Real and imaginary parts of the (non-matched) voltage $V_{\text{NM}}(z)$ and normalised current $Z_0 I_{\text{NM}}(z)$ for the plane wave incidence shown in Figure 15, at frequency 60 MHz (or $L/\lambda = 1/16$), but for loads $Z_L = Z_0/2$ and $Z_R = 2Z_0$, or $\Gamma_L = -1/3$ and $\Gamma_R = 1/3$. The continuous line is the analytic solution, i.e., Eq. (71) plus correction (73) and Eq. (72) plus correction (74) and the stars are the ANSYS simulation results.

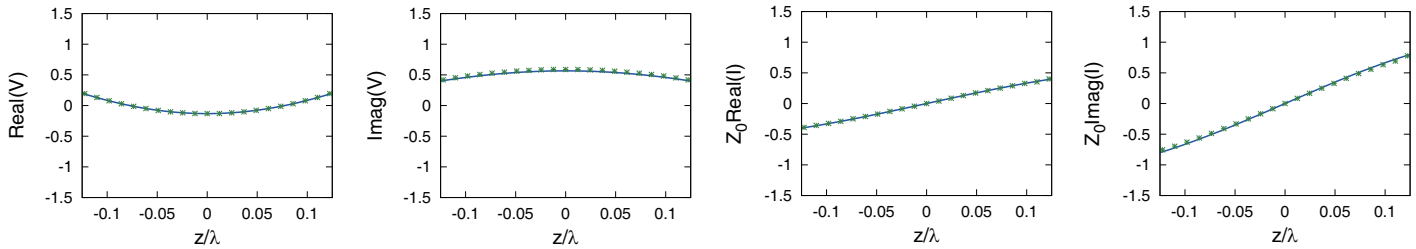

FIGURE 24. Same as Figure 23 for $Z_L = Z_R = Z_0/2$ or $\Gamma_L = \Gamma_R = -1/3$.

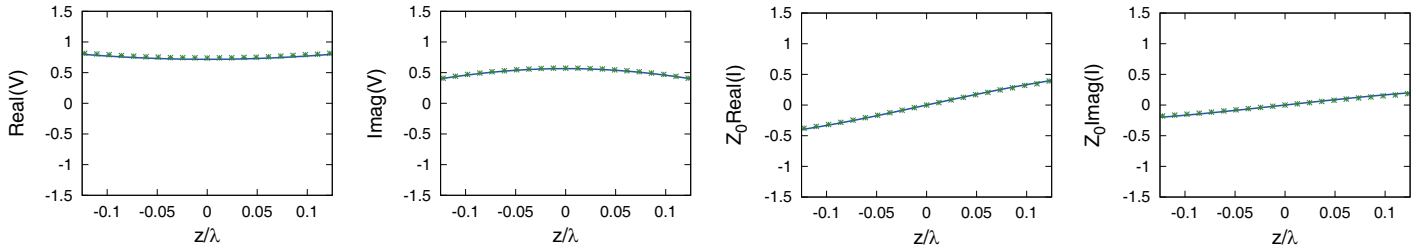

FIGURE 25. Same as Figure 23 for $Z_L = Z_R = 2Z_0$ or $\Gamma_L = \Gamma_R = 1/3$.

where for the second expression we used Eq. (3). Using Eqs. (7), (77), and (78), $Z_0 I_s$ in Eq. (16) comes out

$$Z_0 I_s = jkV^+(\sin\alpha\sin\varphi - \cos\alpha\cos\theta\cos\varphi)e^{jkz\cos\theta}, \quad (79)$$

To derive the H_y component of the incident field, we note that the H components of the incident plane wave are:

$$H_\theta = \frac{E_\varphi}{\eta_0}; \quad H_\varphi = -\frac{E_\theta}{\eta_0} \quad (80)$$

Using the unit vectors identity $\hat{\mathbf{y}} = \hat{\mathbf{r}}\sin\theta\sin\varphi + \hat{\boldsymbol{\theta}}\cos\theta\sin\varphi + \hat{\boldsymbol{\varphi}}\cos\varphi$, given that the incident H field has only θ and φ components, the y component of H (at origin) is

$$H_y = H_\theta\cos\theta\sin\varphi + H_\varphi\cos\varphi$$

$$= \frac{1}{\eta_0}[E_\varphi\cos\theta\sin\varphi - E_\theta\cos\varphi], \quad (81)$$

where in the second expression we used Eq. (80). Using Eqs. (3) and (7), this can be rewritten as

$$\eta_0 H_y = V^+[\sin\alpha\cos\theta\sin\varphi - \cos\alpha\cos\varphi], \quad (82)$$

Using Eqs. (77), V_s in Eq. (15) comes out

$$V_s = jkV^+[\sin\alpha\cos\theta\sin\varphi - \cos\alpha\cos\varphi]e^{jkz\cos\theta}, \quad (83)$$

Here, it is left to show that Eqs. (79) and (83) equal the LHS of Eqs. (14) and (13), respectively, applied on the double-matched solution $V(z)$, $I(z)$ given in Eqs. (30), (38). We start with two intermediate results for the functions $f_1(z)$ and $f_2(z)$ defined in Eq. (23):

$$df_1/dz + jkf_1 = k\cos^2(\theta/2)e^{jkz\cos\theta}$$

$$df_2/dz - jkf_2 = -k\sin^2(\theta/2)e^{jkz\cos\theta}, \quad (84)$$

and obtain

$$\frac{dV}{dz} + jk(Z_0 I) = -jkV^+[\cos^2(\theta/2)\cos(\varphi+\alpha)$$

$$+ \sin^2(\theta/2)\cos(\varphi-\alpha)]e^{jkz\cos\theta} \quad (85)$$

$$Z_0\frac{dI}{dz} + jkV = jkV^+[\sin^2(\theta/2)\cos(\varphi-\alpha)$$

$$- \cos^2(\theta/2)\cos(\varphi+\alpha)]e^{jkz\cos\theta} \quad (86)$$

Using simple trigonometric identities one finds that results (85) and (86) are identical to Eqs. (83) and (79), respectively.

To conclude, this subsection proves that our results are completely compatible with [2–7] *without the need for individual comparisons*. It has been brought for completeness, where individual comparisons with full wave HFSS have been shown in the previous subsection.

6. THE POWER TRANSFERRED TO THE LOADS

We calculate here the power transferred to the loads for the general case of loads Z_L and Z_R as shown in Figure 1, but we start with the simpler double-matched case and therefore need the voltage and current for this case at the terminations ($z = \pm L$). From Eqs. (30) and (38) we obtain

$$V(-L) = jV^+e^{-jkL}\sin[2kL\sin^2(\theta/2)]\cos(\varphi-\alpha) \quad (87)$$

$$V(L) = -jV^+e^{-jkL}\sin[2kL\cos^2(\theta/2)]\cos(\varphi+\alpha) \quad (88)$$

and

$$Z_0 I(-L) = -V(-L); \quad Z_0 I(L) = V(L) \quad (89)$$

satisfy the boundary conditions. From Eqs. (87)–(89), the powers on the "left" and "right" loads for the *double-matched* case are

$$P_L \equiv -V(-L)I^*(-L)$$

$$= \frac{|V^+|^2}{Z_0}\sin^2[2kL\sin^2(\theta/2)]\cos^2(\varphi-\alpha) \quad (90)$$

$$P_R \equiv V(L)I^*(L)$$

$$= \frac{|V^+|^2}{Z_0}\sin^2[2kL\cos^2(\theta/2)]\cos^2(\varphi+\alpha) \quad (91)$$

Before generalising, we shall interpret those results with the aid of the radiation properties of the TL in [1]. The TL at origin is hit by the plane wave moving toward it at polarisation given in Eq. (2), shown in Figure 2. The polarisation of the radiation from a matched TL, having a source at its left (as in Figure 26) is known from [1] and given by

$$\hat{\mathbf{p}}^+(\theta,\varphi) = \hat{\boldsymbol{\theta}}\cos\varphi + \hat{\boldsymbol{\varphi}}\sin\varphi, \quad (92)$$

which equals the incident wave polarisation for $\alpha = \varphi$. This polarisation maximizes the power P_L into the left load of a double-matched TL, given in Eq. (90), while a polarisation orthogonal to $\hat{\mathbf{p}}^+$ results in $P_L = 0$. This power is proportional to $\sin^2[2kL\sin^2(\theta/2)]$, according to the radiation pattern of a TL carrying a forward wave only (see Subsection 2.1 in [1]). This suggests that P_L, i.e., the power into the left load for the

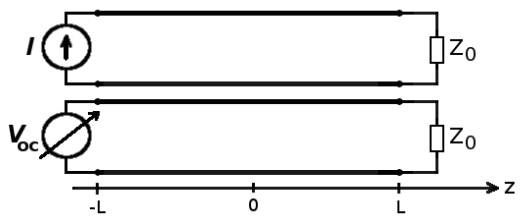

FIGURE 26. Upper panel: radiating TL fed by a current source I at $z = -L$, matched at $z = L$. Lower panel: the same TL in receive mode, with a voltmeter at $z = -L$ measuring the open circuit voltage V_{oc}.

double-matched TL, is closely related to the transmitting properties of a source at the left termination, issuing a forward wave, as explained in Appendix C.

Similarly, P_R is proportional to $\sin^2[2kL\cos^2(\theta/2)]$, according to the radiation pattern of a TL carrying a backward wave only and maximised for the polarisation radiated in this case

$$\widehat{\mathbf{p}}^-(\theta,\varphi) = \hat{\boldsymbol{\theta}}\cos\varphi - \hat{\boldsymbol{\varphi}}\sin\varphi, \tag{93}$$

i.e., $\alpha = -\varphi$ (see Subsection 2.2 in [1]). Also $P_R = 0$ for a polarisation orthogonal to $\widehat{\mathbf{p}}^-$. This suggests that P_R, i.e., the power into the right load for the double-matched TL, is closely related to the transmitting properties of a source at the right termination, issuing a backward wave.

We now generalise the powers for a TL with any loads. We set $z = \pm L$ in Eqs. (48), (54) , obtaining

$$V_{\text{NM}}(-L) = (1+\Gamma_L)\frac{\Gamma_R e^{-j2kL}V(L)+V(-L)}{1-\Gamma_L\Gamma_R e^{-j4kL}} \tag{94}$$

$$V_{\text{NM}}(L) = (1+\Gamma_R)\frac{\Gamma_L e^{-j2kL}V(-L)+V(L)}{1-\Gamma_L\Gamma_R e^{-j4kL}} \tag{95}$$

and

$$Z_L I_{\text{NM}}(-L) = -V_{\text{NM}}(-L); \quad Z_R I_{\text{NM}}(L) = V_{\text{NM}}(L) \tag{96}$$

satisfy the boundary conditions.

Now we express the power on the "left" load Z_L by $P_{\text{NM,L}} = Re\{-V_{\text{NM}}(-L)I^*_{\text{NM}}(-L)\}$ and on the "right" load Z_R by $P_{\text{NM,R}} = Re\{V_{\text{NM}}(L)I^*_{\text{NM}}(L)\}$. Using Eqs. (94)-(96) one obtains

$$P_{\text{NM,L}} = \frac{1-|\Gamma_L|^2}{|1-\Gamma_L\Gamma_R e^{-j4kL}|^2}[P_L + |\Gamma_R|^2 P_R - 2P_{\text{mix}}Re\{\Gamma_R e^{-j2kL}\}] \tag{97}$$

$$P_{\text{NM,R}} = \frac{1-|\Gamma_R|^2}{|1-\Gamma_L\Gamma_R e^{-j4kL}|^2}[P_R + |\Gamma_L|^2 P_L - 2P_{\text{mix}}Re\{\Gamma_L e^{-j2kL}\}]. \tag{98}$$

The generalised results for the powers are expressed in terms of the double-matched powers P_L and P_R (given in Eqs. (90)-(91)) plus an additional "mixed" term P_{mix} given by

$$P_{\text{mix}} \equiv V(L)I^*(-L) \equiv -V(-L)I^*(L)$$

$$\frac{|V^+|^2}{Z_0}\sin[2kL\sin^2(\theta/2)]\sin[2kL\cos^2(\theta/2)] = \cos(\varphi-\alpha)\cos(\varphi+\alpha) \tag{99}$$

The general non-matched case given in Eqs. (97)-(98) is affected by both radiation patterns and polarisations, and their combination is found in the mixed term in Eq. (99). We remark that for a polarisation orthogonal to either $\widehat{\mathbf{p}}^+$ or $\widehat{\mathbf{p}}^-$, $P_{\text{mix}} = 0$ and either P_L or P_R is 0, in which case the received powers are according to either $\sin^2[2kL\cos^2(\theta/2)]$ or $\sin^2[2kL\sin^2(\theta/2)]$.

The formal connection between the transmitting and receiving properties of TL, i.e., the reciprocity, is analysed in the next section.

7. CONSISTENCY BETWEEN TRANSMITTING-RECEIVING RADIATION PROPERTIES

To analyse the connection between the results of receiving electromagnetic radiation shown in this work and the results of transmitting (radiating) electromagnetic radiation in [1], we have to summarise below some results from [1] and rewrite them in a convenient form. We shall refer to Appendix C in which we summarise some properties of TL as antennas and the reciprocity between radiation and absorption. As explained in Appendix C, the reciprocity will be tested separately for the "left" and "right" ports.

The far electric field radiated by a TL carrying a forward wave only as in the upper panel of Figure 26, (calculated in Subsection 2.1 of [1]) is given in Eq. (A1) in terms of the value of I^+ in the middle of the TL at $z = 0$. We rewrite it here in terms of the current source I (at $z = -L$) in the standard form for a radiating antenna fed by a current as given in Eq. (C2), from which obtain the effective antenna length for the radiation of a TL carrying a forward wave only, hence we use a "+" superscript

$$\mathbf{l}^+_{\text{eff}} = 2jde^{-jkL}\sin[2kL\sin^2(\theta/2)]\widehat{\mathbf{p}}^+ \tag{100}$$

where the polarisation vector $\widehat{\mathbf{p}}^+$ is defined in Eq. (92).

Note that this is the function $f_2(-L)$ defined in (23), times $2jd$ times the unit vector $\widehat{\mathbf{p}}^+$. The factor "2" is because (C3) yields the open port voltage which is twice of the matched voltage in (30), for which f_2 has been defined, and "d" gives the dimensions of length, which multiplied by the incident field is V^+ in (7). The "j" could have been added to the definitions of $f_{1,2}$ and removed from (30), and the unit vector $\widehat{\mathbf{p}}^+$ is the polarisation of the forward wave radiation in [1], hence the direction of l^+_{eff} as shown in (C2).

The radiation resistance for this case (given in Eq. (36) of [1]) is

$$r_{\text{rad}} = \frac{\eta_0}{2\pi}(kd)^2\left[1-\text{sinc}(4kL)\right], \tag{101}$$

which does not need a "+" superscript, being valid also for a backward wave only. The radiation pattern (directivity) for a forward wave only is given in Subsection 2.1, Eq. (13) in [1] and satisfies the relation (C4). It is

$$D^+(\theta) = 2\frac{\sin^2[2kL\sin^2(\theta/2)]}{[1-\text{sinc}(4kL)]}. \tag{102}$$

When dealing with radiation from TL, which is usually small relative to the power carried by the TL, we may use the term "radiation losses" for the power lost to radiation. So in the upper panel of Figure 26, the radiated power is $|I|^2 r_{\text{rad}}$, and the power transmitted by the TL is $|I|^2 Z_0$, and clearly $r_{\text{rad}} \ll Z_0$. But in the context of the radiating properties we have to consider the radiation efficiency (explained in Appendix C), defined as the radiated power, divided by the total power into the antenna. In our case this is

$$\eta = \frac{r_{\text{rad}}}{r_{\text{rad}} + Z_0} \simeq \frac{r_{\text{rad}}}{Z_0}. \tag{103}$$

which is small, meaning that the (matched) TL is not an efficient antenna. Eq. (103) is valid for both forward only or backward only waves, hence does not need a superscript. The antenna gain is the directivity multiplied by the efficiency (explained in Appendix C) and comes out

$$G^+(\theta) = \frac{(kd)^2 \eta_0 \sin^2[2kL\sin^2(\theta/2)]}{\pi Z_0}, \tag{104}$$

Now, in receiving mode, we may use (C3) to obtain the open circuit voltage measured in the lower panel of Figure 26

$$V_{\text{oc}} = \mathbf{E} \cdot \mathbf{l}^+_{\text{eff}} = 2jE_0\, d e^{-jkL} \sin[2kL\sin^2(\theta/2)] \cos(\varphi - \alpha), \tag{105}$$

which is compared with the open end voltage obtained from the formalism developed in this work. So using Eq. (94) with $\Gamma_R = 0$ and $\Gamma_L = 1$ (open) yields exactly the result (105) where we identify $V^+ = E_0\, d$ according to Eq. (7). Also the open circuit voltage in (105) is twice of the double-matched voltage (30) at $z = -L$, as expected. The absolute value of V_{oc} is maximal for a matched polarisation, i.e., for $\alpha = \varphi$.

We replace now the voltmeter in the lower panel of Figure 26 by a load Z_L (left). Eq. (97) reduces for $\Gamma_R = 0$ to $P_{\text{NM,L}} = (1 - |\Gamma_L|^2)P_L$, so maximum power is obtained for $\Gamma_L = 0$ ($Z_L = Z_0$), yielding Eq. (90). Using the matched polarisation ($\alpha = \varphi$) in (90) results in the maximum received power:

$$P_{\text{rec}} = \frac{|V^+|^2}{Z_0} \sin^2[2kL\sin^2(\theta/2)]. \tag{106}$$

Dividing this by the Poynting vector $S = E_0^2/\eta_0$ results in the effective receiving cross section area A^+ (for receiving into the left termination - the equivalent of transmitting a forward wave)

$$A^+ = \frac{P_{\text{rec}}}{S} = \frac{d^2\eta_0}{Z_0} \sin^2[2kL\sin^2(\theta/2)]. \tag{107}$$

which together with Eq. (104) satisfies (C1).

A similar analysis for the backward wave, using the current source at the $z = L$ termination (pointing upward) and the matched load at $z = -L$ in Figure 26 (using Eq. (A2)) yields the field radiated by a backward wave current from which we obtain via Eq. (C2) the effective antenna length for the radiation of a TL carrying a backward wave only

$$\mathbf{l}^-_{\text{eff}} = -2jde^{-jkL} \sin[2kL\cos^2(\theta/2)]\widehat{\mathbf{p}}^-, \tag{108}$$

where the polarisation vector $\widehat{\mathbf{p}}^-$ is defined in Eq. (93).

This is the function $f_1(L)$ defined in (23), times $-2jd$ times the unit vector $\widehat{\mathbf{p}}^-$. The interpretation of l^-_{eff} is similar to the one given for l^+_{eff}, and the extra "minus" is because the field in [1] is expressed by a current defined to right in the "upper" conductor, and the current source feeding the "right" port is defined "up".

For this case, the gain is the directivity function D^- given in Eq. (17) of [1] multiplied by the efficiency in Eq. (103), which yields

$$G^-(\theta) = \frac{(kd)^2 \eta_0 \sin^2[2kL\cos^2(\theta/2)]}{\pi Z_0}, \tag{109}$$

The effective receiving cross section area A^- comes out

$$A^- = \frac{d^2\eta_0}{Z_0} \cos^2[2kL\cos^2(\theta/2)], \tag{110}$$

which together with Eq. (109) satisfies (C1).

8. CONCLUSION

We have derived in this work the voltage and differential current developed on an ideal two-conductors TEM transmission line (TL) of any small electric cross section, connected to passive loads and hit by a monochromatic plane wave, as shown in Figure 1.

For this derivation we used our knowledge on the radiation properties of TL [1] to build S matrices which describe the radiating system and used the reciprocity to derive the current and voltage induced on the TL. This methodology allowed us to derive first the voltage and current on a double-matched TL, yielding the relatively *simple* expressions given in Eqs. (30) and (38). As mentioned before, the simple and interpretable expression for the double-matched case is one of the advantages of our methodology. The generalisation to any loads is then obtained, using the S matrix.

We validated our analytic results in Section 5.1 for both the double-matched TL case and the non-matched case for different plane wave incidences. We also showed in Section 5.2 that our analytic results are compatible with the methodology used in previous works [2–7]. The simplicity of this proof, requiring the application of Eqs. (13) and (14) *only* on the double-matched solution (see Eq. 75), emphasises the *added value* of this work.

In Section 6, we derived the powers on the loads and showed the connection between those powers and the radiating properties of the TL. For the double-matched TL, the power on the "left" load has the same spatial dependence on the incident plane wave direction as the radiation pattern of a forward wave and is maximised for the polarisation of a radiating forward wave $\widehat{\mathbf{p}}^+$ (see Eq. (92)). Similarly, for the double-matched TL, the power on the "right" load has the same spatial dependence on the incident plane wave direction as the radiation pattern of a backward wave and is maximised for the polarisation $\widehat{\mathbf{p}}^-$ (see Eq. (93)). The general non-matched case is affected by both radiation patterns and polarisations, and their combination is found in a mixed term.

In Section 7, we showed that the formal relations between receiving cross section area and antenna gain are satisfied for the

TL, making this article the first one to explicitly show that the reciprocity for TL radiation/absorption is satisfied. Although it is clear from electromagnetic theory that reciprocity holds in this case, it has never been used for calculations in similar TL configurations. For example, [2] deals with the reciprocal of [16] (published 14 years earlier). Not only has this reciprocity not been used or tested for, but also [16] has not been referenced in [2]. In this work, reciprocity has been used to explain the physical meaning of the results. To be mentioned that the formalism elaborated in this work is applicable to any configuration for which one aims to obtain the receiving characteristics from the radiation characteristics, and we already applied it successfully for the Quasi-TEM insulated transmission lines [14], which is applicable to microstrips — to be published.

The algorithm can also be applied to multiconductor transmission lines (MTL). Practical MTL (for which the field lines extend beyond the insulator) of N conductors develop $N-1$ modes. Each mode has its own characteristic impedance and its own propagation delay. In case of uniform medium (air or "infinite" insulator), there are still $N-1$ degenerate modes, all with the same propagation delay, like in [5]. We dealt in the past with MTL for a different problem [17, 18], developing a robust algorithm to obtain the properties of the modes. It is reasonable to treat radiation/absorption of MTL using a per mode analysis for the reciprocity between radiation and absorption.

APPENDIX A. FAR RADIATED E FIELD AND ITS NORMALISATION

The purpose of this appendix is to summarise some results from [1] needed in Sections 3 and 7 and pave the way to defining consistently the S matrices.

In case the far (test) antennas (named θ and φ) in Figures 3 and 4 are not fed, and the TL is fed at its terminations, it radiates a **spherical far field**. This field is sensed by each test antenna issuing a voltage V^- to a matched load. On the other hand, the TL as receiving antenna is hit by a **plane wave**, which we present by an incoming voltage V^+, as given in Eq. (7).

For reciprocity to be satisfied, we have to correctly connect the above radiated **spherical far field** with the absorbed **plane wave** hitting the antenna. This means that the above voltage V^-, when fed to the same (test) antenna (called now V^+), generates the same far field at the TL location as this plane wave hitting our TL.

Two results from [1] are presented here: A TL between $[-L, L]$ on the z axis, carrying a forward current only I^+ (specified at $z=0$), radiates:

$$\mathbf{E}^+ = -\eta_0 G(r) 2kdI^+ \sin\left[2kL\sin^2(\theta/2)\right][\hat{\boldsymbol{\theta}}\cos\varphi + \hat{\boldsymbol{\varphi}}\sin\varphi]. \tag{A1}$$

A TL between $[-L, L]$ on the z axis, carrying a backward current only I^- (specified at $z=0$, and **defined to the right**), radiates:

$$\mathbf{E}^- = -\eta_0 G(r) 2kdI^- \sin\left[2kL\cos^2(\theta/2)\right][\hat{\boldsymbol{\theta}}\cos\varphi - \hat{\boldsymbol{\varphi}}\sin\varphi]. \tag{A2}$$

Adequate combinations of those results, separated into components E_θ and E_φ, are used in Section 3 to derive the θ and φ terms of the S matrices describing the circuits in Figures 6 and 7. Therefore, those radiated fields have to be scaled into outgoing voltages V_θ^- and V_φ^- for the circuit in Figures 6 and to outgoing currents I_θ^- and I_φ^- for the circuit in Figures 7, and we calculate here those scaling factors.

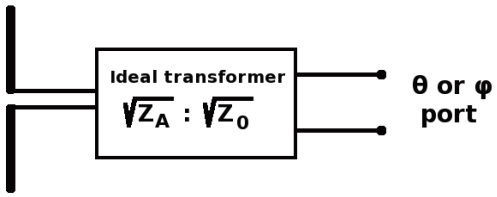

FIGURE A1. The antenna model assumes a real antenna impedance Z_A matched by an ideal transformer to the θ or φ port of impedance Z_0.

The ports θ and φ have been defined for the impedance Z_0, which is the characteristic impedance of the analysed TL. To make those ports matched, we use the antenna model shown in Figure A1. The model assumes a real antenna impedance Z_A matched via an ideal transformer to the θ or φ port of impedance Z_0. Using the effective length of the antenna l_{eff} (for the given incidence direction), one expresses the open circuit voltage on the antenna $V_{\text{oc}} = E\, l_{\text{eff}}$ (see [10] or Eq. (C3)) where E is E_θ or E_φ. With the θ or φ port being matched, the antenna "sees" a matched load, so that the actual voltage on the antenna terminals is $V_{\text{oc}}/2$, and the outgoing voltage at the port (θ or φ) is

$$V^- = \frac{1}{2} E\, l_{\text{eff}} \sqrt{Z_0/Z_A}. \tag{A3}$$

Now to activate the antenna in transmitting mode, we feed the θ or φ port by V^+, so the voltage at the antenna terminals is $V^+\sqrt{Z_A/Z_0}$, divided by Z_A to obtain the current feeding the antenna:

$$I_A = V^+/\sqrt{Z_A Z_0} \tag{A4}$$

Using the well-known formula for the far E-field radiated by a dipole $E_0 = jk\eta_0 G(r) I_A l_{\text{eff}}$ (see [10] or Eq. (C2)), where l_{eff} is the effective dipole length discussed before, into the same direction. The field radiated from the antenna(s) has been named E_0 to distinguish it from the previously discussed field travelling toward the antenna(s). Expressing it as function of V^+, we obtain

$$E_0 = jk\eta_0 G(r) l_{\text{eff}} V^+/\sqrt{Z_A Z_0} \tag{A5}$$

This field E_0, radiated from the far antenna(s), is the field incident on the TL (or one of its components), mentioned in Figure 2, and as explained at the beginning of this appendix it is the intensity of the hitting plane wave. We therefore normalize it so that $E_0\, d = V^+$ (see Eq. (7)), considering the field incident on the TL as plane wave. Imposing condition (7) on Eq. (A5) results in

$$l_{\text{eff}} = \frac{\sqrt{Z_A Z_0}}{jk\eta_0 G(r) d} \tag{A6}$$

Given that the far antennas are only tools to build the S matrices and from them infer the voltage and current along the TL, the "actual" value of l_{eff} is of no interest, so to express the fields

radiated by the TL E_θ and E_φ as voltages, we set l_{eff} from (A6) into Eq. (A3), obtaining

$$V^-_{\theta \text{ or } \varphi} = \frac{Z_0 E_{\theta \text{ or } \varphi}}{2jk\eta_0 G(r) d} \tag{A7}$$

For the case that we need to express the fields radiated by the TL E_θ and E_φ as outgoing currents, we use $I^- = -V^-/Z_0$, obtaining:

$$I^-_{\theta \text{ or } \varphi} = -\frac{E_{\theta \text{ or } \varphi}}{2jk\eta_0 G(r) d} \tag{A8}$$

APPENDIX B. GENERALIZED SCATTERING MATRIX

In this appendix we define the generalized scattering matrix [8] and explain its reciprocity properties. For more details, see Subsection 4.3 in [8]. The generalized scattering matrix for an arbitrary network (as shown in Figure B1) is defined by the following matrix equation

$$\mathbf{V}^- = \mathbf{S}\mathbf{V}^+, \tag{B1}$$

where $\mathbf{V}^\pm$ are column vectors for the incoming and outgoing voltage waves at the ports of the network, and each port has its own characteristic impedance, as shown in Figure B1. The voltage and current waves at the ports satisfy

$$\mathbf{V}^+ = \mathbf{Z}\mathbf{I}^+; \quad \mathbf{V}^- = -\mathbf{Z}\mathbf{I}^-, \tag{B2}$$

where $\mathbf{Z}$ is a diagonal matrix of the characteristic impedances in Figure B1:

$$Z_{ij} = Z_i \delta_{ij}, \tag{B3}$$

so one can easily apply functions on them, as follows.

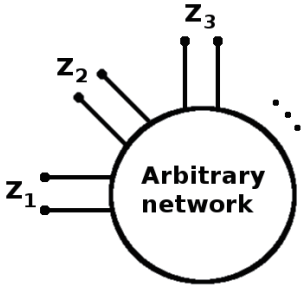

FIGURE B1. An N ports arbitrary network interfaced to transmission lines of characteristic impedances $Z_1, Z_2, \ldots Z_N$.

Normalizing the voltages and currents at each port according to

$$\mathbf{a}^\pm \equiv \sqrt{\mathbf{Z}^{-1}}\mathbf{V}^\pm; \quad \mathbf{b}^\pm \equiv \sqrt{\mathbf{Z}}\mathbf{I}^\pm, \tag{B4}$$

and setting into Eq. (B1) result in

$$\mathbf{a}^- = \sqrt{\mathbf{Z}^{-1}}\mathbf{S}\sqrt{\mathbf{Z}}\mathbf{a}^+, \tag{B5}$$

which define the (ordinary) scattering matrix, for which we use a lower case "s"

$$\mathbf{s} \equiv \sqrt{\mathbf{Z}^{-1}}\mathbf{S}\sqrt{\mathbf{Z}}. \tag{B6}$$

It is known [8–13] that the reciprocity condition for the ordinary scattering matrix is

$$s_{ij} = s_{ji}. \tag{B7}$$

Using this in Eq. (B6) results in the reciprocity condition for the generalized scattering matrix

$$S_{ij} Z_j = S_{ji} Z_i \tag{B8}$$

Scattering matrices are usually defined for voltage waves, but in this work we need to define a generalized scattering matrix for current waves as follows

$$\mathbf{I}^- = \mathbf{S}_I \mathbf{I}^+, \tag{B9}$$

and we name it $\mathbf{S}_I$ to distinguish it from the regular scattering matrix in (B1). Using Eq. (B2), one obtains

$$\mathbf{V}^- = -\mathbf{Z}\mathbf{S}_I\mathbf{Z}^{-1}\mathbf{V}^+. \tag{B10}$$

Comparing it with (B1) we get the relation

$$\mathbf{S} = -\mathbf{Z}\mathbf{S}_I\mathbf{Z}^{-1}. \tag{B11}$$

Setting it in (B6) results in

$$\mathbf{s} = -\sqrt{\mathbf{Z}}\mathbf{S}\sqrt{\mathbf{Z}^{-1}}, \tag{B12}$$

and using (B7) we obtain

$$S_{I\,ij} Z_i = S_{I\,ji} Z_j \tag{B13}$$

APPENDIX C. TL AS TRANSMITTING OR RECEIVING ANTENNAS AND RECIPROCITY

A TL can be fed in principle by two *independent* sources, one at each termination port. The "left" port at $z = -L$ generates the forward wave, and the "right" port at $z = L$ generates the backward wave. Dealing with two ports, the reciprocity holds for each port *separately*, and we summarise here the reciprocity principles for a *given* port. The best known reciprocity relation is

$$A(\theta, \varphi) = \frac{\lambda^2}{4\pi} G(\theta, \varphi) \tag{C1}$$

where A is the effective area for receiving, defined as the power delivered to a matched load divided by the incoming Pointing vector; λ is the wavelength; and G is the radiating antenna gain. G is best understood as the antenna directivity D multiplied by the antenna efficiency: $G(\theta, \varphi) = \eta D(\theta, \varphi)$, where the antenna efficiency η is the ratio of radiated power over the power supplied to the antenna. The antenna directivity D, multiplied by the average *radiated* power per unit area, yields the actual far pointing vector at the spherical coordinates θ, φ.

Another important function very useful for antennas fed at a port is the *effective length* function $\mathbf{l}_{\text{eff}}(\theta, \varphi)$. For a transmitting antenna it is used to express the far radiated E-field

$$\mathbf{E} = jk\eta_0 G(r) I \mathbf{l}_{\text{eff}}(\theta, \varphi), \tag{C2}$$

where I is the current supplied to the antenna port, $\eta_0 = 377\ [\Omega]$ the free space impedance, and $G(r) = \frac{e^{-jkr}}{4\pi r}$ the Green function. For a receiving antenna it is used to calculate the voltage at the open port

$$V_{\text{oc}} = \mathbf{E_0} \cdot \mathbf{l}_{\text{eff}}(\theta, \varphi), \tag{C3}$$

where $\mathbf{E_0}$ is the intensity of the plane wave hitting the antenna. Although not directly evident from the above definitions, reciprocity implies that $\mathbf{l}_{\text{eff}}$ is the *same function* for the radiating

case in (C2) as for the receiving case in (C3). In fact, the functions G, D, and A are all proportional to $|\mathbf{l}_{\text{eff}}|^2$, and this proportionality sustains Eq. (C1). Given the antenna radiation resistance r_{rad}, the proportionality of D is

$$D(\theta,\varphi) = \frac{\eta_0 k^2}{4\pi r_{\text{rad}}} |\mathbf{l}_{\text{eff}}|^2 \tag{C4}$$

from which one infers the proportionality of G and A.

The reciprocity is very convenient and useful. For an antenna fed by the current I, one typically derives the far radiated E-field and expresses it in the form of (C2), obtaining the function $\mathbf{l}_{\text{eff}}(\theta,\varphi)$. This may be used in receiving mode to calculate the open port voltage via (C3), and from it the voltage or power for any load at the port.

ACKNOWLEDGEMENT

This work has been partially supported by the Israeli Science Foundation (ISF).

REFERENCES

[1] Ianconescu, R. and V. Vulfin, "Radiation from free space TEM transmission lines," *IET Microwaves, Antennas & Propagation*, Vol. 13, No. 13, 2242–2255, 2019.

[2] Taylor, C., R. Satterwhite, and C. Harrison, "The response of a terminated two-wire transmission line excited by a nonuniform electromagnetic field," *IEEE Transactions on Antennas and Propagation*, Vol. 13, No. 6, 987–989, 1965.

[3] Smith, A. A., "A more convenient form of the equations for the response of a transmission line excited by nonuniform fields," *IEEE Transactions on Electromagnetic Compatibility*, Vol. EMC-15, No. 3, 151–152, 1973.

[4] Harrison, C. W., "Generalized theory of impedance loaded multiconductor transmission lines in an incident field," *IEEE Transactions on Electromagnetic Compatibility*, Vol. EMC-14, No. 2, 56–63, 1972.

[5] Paul, C. R., "Frequency response of multiconductor transmission lines illuminated by an electromagnetic field," *IEEE Transactions on Electromagnetic Compatibility*, Vol. EMC-18, No. 4, 183–190, 1976.

[6] Agrawal, A. K., H. J. Price, and S. H. Gurbaxani, "Transient response of multiconductor transmission lines excited by a nonuniform electromagnetic field," *IEEE Transactions on Electromagnetic Compatibility*, Vol. EMC-22, No. 2, 119–129, 1980.

[7] Smith, A. A., *Coupling of External Electromagnetic Fields to Transmission Lines*, Wiley, 1977.

[8] Pozar, D. M., *Microwave Engineering*, Wiley, 2009.

[9] Collin, R. E., *Antennas and Radiowave Propagation*, McGraw-Hill, 1985.

[10] Orfanidis, S. J., *Electromagnetic Waves and Antennas*, ISBN: 0130938556, Rutgers University, 2002.

[11] Ramo, S., J. R. Whinnery, and T. V. Duzer, *Fields and Waves in Communication Electronics*, 3rd ed., John Wiley & Sons, 1994.

[12] Jordan, E. C. and K. G. Balmain, *Electromagnetic Waves and Radiating Systems*, 2nd ed., Prentice Hall, 1968.

[13] Balanis, C. A., *Antenna Theory: Analysis and Design*, John Wiley & Sons, 2016.

[14] Ianconescu, R. and V. Vulfin, "Radiation from quasi-TEM insulated transmission lines," *IET Microwaves, Antennas & Propagation*, Vol. 13, No. 6, 761–773, 2019.

[15] Manneback, C., "Radiation from transmission lines," *Transactions of the American Institute of Electrical Engineers*, Vol. XLII, 289–301, 1923.

[16] Storer, J. E. and R. King, "Radiation resistance of a two-wire line," *Proceedings of the IRE*, Vol. 39, No. 11, 1408–1412, 1951.

[17] Vulfin, V. and R. Ianconescu, "Transmission of the maximum number of signals through a multiconductor transmission line without crosstalk or return loss: Theory and simulation," *IET Microwaves, Antennas & Propagation*, Vol. 9, No. 13, 1444–1452, 2015.

[18] Ianconescu, R. and V. Vulfin, "Analysis of lossy multiconductor transmission lines and application of a crosstalk cancelling algorithm," *IET Microwaves, Antennas & Propagation*, Vol. 11, No. 3, 394–401, 2017.